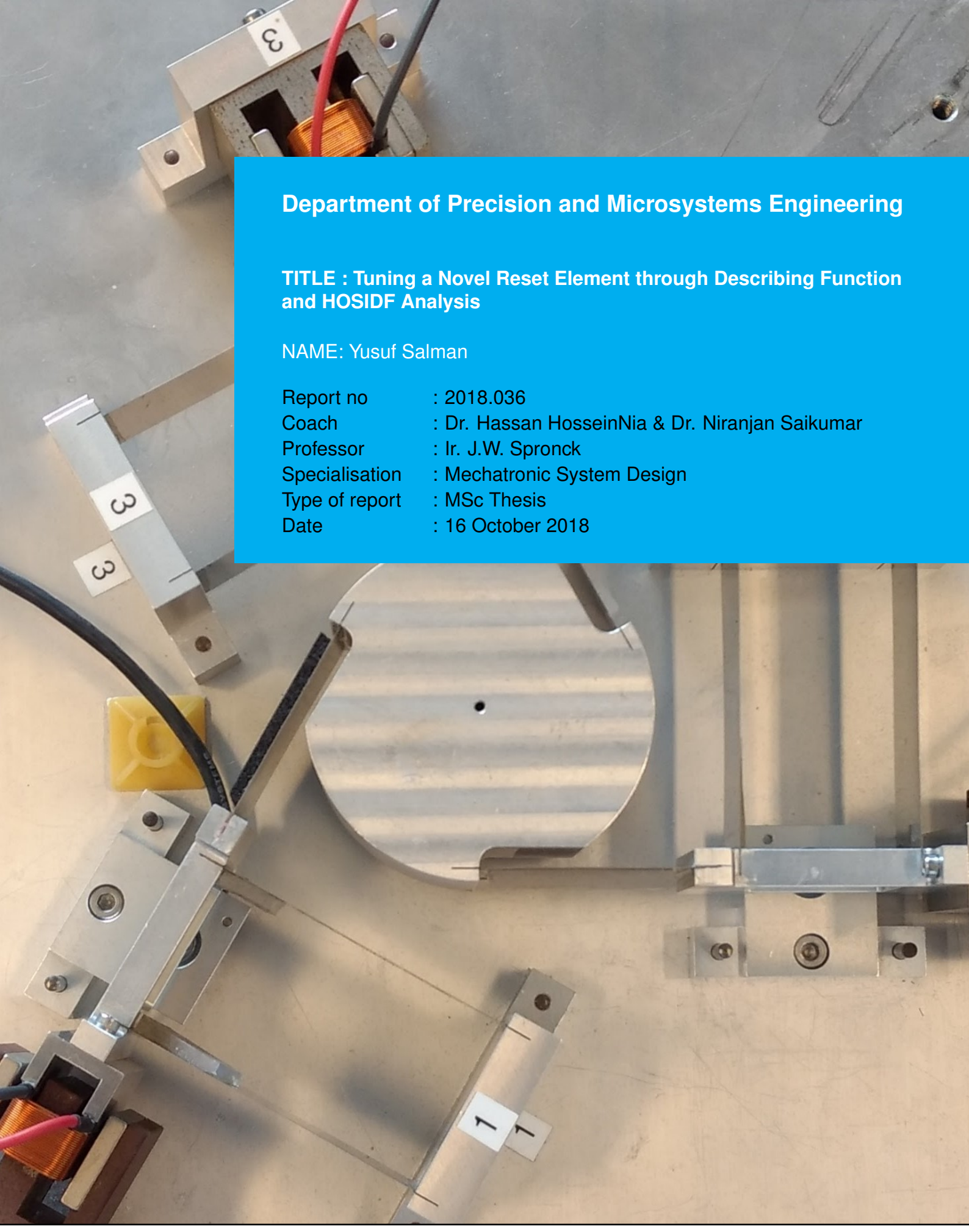

Department of Precision and Microsystems Engineering

TITLE : Tuning a Novel Reset Element through Describing Function and HOSIDF Analysis

NAME: Yusuf Salman

Report no	: 2018.036
Coach	: Dr. Hassan HosseinNia & Dr. Niranjan Saikumar
Professor	: Ir. J.W. Spronck
Specialisation	: Mechatronic System Design
Type of report	: MSc Thesis
Date	: 16 October 2018

TUNING A NOVEL RESET ELEMENT

THROUGH DESCRIBING FUNCTION AND HOSIDF ANALYSIS

by

Yusuf Salman

in partial fulfillment of the requirements for the degree of

Master of Science
in Mechanical Engineering

at the Delft University of Technology,
to be defended publicly on Wednesday 31 October, 2018 at 13.00

Student number:	4610962
Supervisor:	Dr. N. Saikumar
	Dr. S. H. HosseinNia
Thesis committee:	Ir. J. W. Spronck (chairman)
	Dr. S. H. HosseinNia
	Dr. ir. J. F. L. Goosen
	Dr. N. Saikumar

An electronic version of this thesis is available at http://repository.tudelft.nl/.

TU Delft Delft University of Technology

PREFACE

This report is the final part which conclude my master study in Precision and Microsystems Engineering track at TU Delft. During my study here, I have gained a lot of knowledge and experience that sharpening my intuition as an engineer. I am so glad I can achieve my dream to obtain a master degree thanks to Indonesia Endowment Fund for Education (LPDP RI) for financing my master study at TU Delft. This thesis would not be completed without the the help of these people, so I would like to thank:

Niranjan Saikumar, thanks for your guidance and patience to help me solve every problem in this thesis. For a year, I learned a lot from you. Your suggestion and advice are priceless. I believe this thesis won't be going anywhere until this current state except with your help.

Hassan HosseinNia, thanks for your support and attention that you gave throughout the year. You are always encouraging me to be optimistic and to give the best of me. It is my pleasure to work under your supervision.

Friends of PME department, especially from Jo and Hassan group, for the discussion, inputs, and inspiration which helped me to evaluate and to improve my work. To Linda, who still answering my questions regarding experiment despite she already graduated.

Lastly, to my family, my Indonesian friends, my housemates at Valkenlaan 36 for the endless care and support. Thanks for being there whenever I need.

Yusuf Salman
Delft, 16 October 2018

ABSTRACT

The high-tech industry is pushing the motion system technology towards faster, more precise and more robust system. One of the keys to this growing demand is the advancement of motion control. To this day, Proportional-Integral-Derivative (PID) has been the workhorse for the industry system control. This is because PID is simple to design and implement and adapt to industrial loopshaping method. Nevertheless, PID suffers fundamental limitations of linear control. To deal with this, a nonlinear control should be utilized. Reset control is a nonlinear control that is still easy but can overcome the limitation of linear control and more importantly, loop shaping method can be used to reset control by using describing function analysis which is pseudo-approximation of nonlinear system that based on the first harmonic. However, reset control also introduces higher order harmonics into the system that can negatively affect system performance. This is because these harmonics may cause some unwanted dynamics present in system response. Describing function which is the common tool to analyze and design reset control is not accurate enough since higher order harmonics are not considered. Recently, a tool to visualize higher order harmonics in frequency domain is developed. This open the possibilities to study the behavior of higher order harmonics and its effect to system performance.

This thesis focuses on a performance analysis and tuning of a novel reset element called 'Constant in Gain,Lead in Phase'(CgLp). It is shown by the literature that reset control is often utilized to provide phase lag reduction but CgLp has shown the use of reset control to provide phase compensation and this improves system performance. Since its introduction, no guidelines available in the literature to design and tune CgLp. Looking at its potential to be industry standard for motion control, finding guidelines to tune CgLp is an important step to achieve this goal. To do the optimal tuning of reset element, higher order harmonics should be considered so that the effect of unwanted response can be minimized while maintaining the advantage of reset control. Therefore, the work in this thesis is performed by doing performance analysis of CgLp through describing function and HOSIDF.

It is shown that while there is an improvement in tracking and steady state precision performance by using CgLp compared to normal PID, there is deterioration of the performance although describing function predicted an improvement. This is because there is a trade-off between improvement by CgLp and the rise of higher order harmonics gain. In this work, the higher order harmonics was considered at the bandwidth frequency and normalized over its first harmonic. It was observed that the optimal performance is achieved when the highest gain value of normalized 3^{rd} harmonic is around half of maximum possible value of normalized 3^{rd} harmonic.

CONTENTS

1

MOTIVATION

Motion control plays an important role in the high tech industry. Be it semiconductor manufacturing, optical scanning or precision machining, high speed positioning system with nanometer precision is a necessity. To achieve this, high performance motion control is required. Good motion control ensures that the overall system has a high bandwidth, tracking and precision while maintaining stability and robustness. The improvement of these performances allows the industry to deliver a higher quality product with reduced production time. For instance, better tracking and precision performance of a wafer stage in lithography machine as shown in Fig.1.1 can increase the number of integrated circuit(IC)s made on a single wafer. This is because with a better tracking, the error during motion is reduced and better precision yields to less error at steady-state. Furthermore, higher bandwidth enables the wafer stage to move faster so the production time can be reduced.

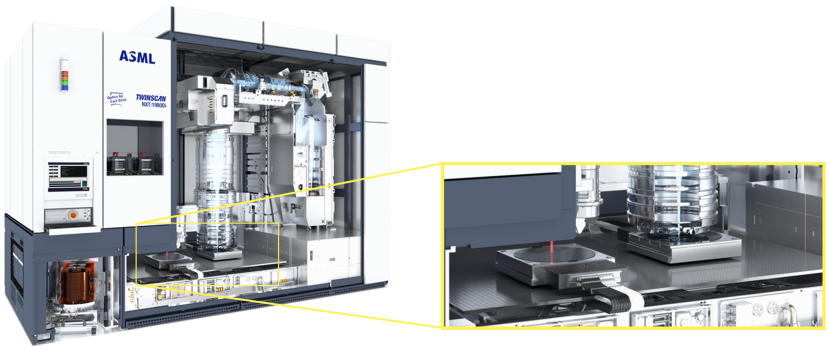

Figure 1.1: Wafer stage in lithography machine [1]

Proportional-Integrator-Derivative(PID) is the industrial standard for system control [2] and has been used for several years even in high-tech precision industry like semiconductor manufacturing. It has been widely used due to its simplicity and ability to provide high bandwidth and robust control. During the design of PID controller, the engineer uses the so-called loop shaping technique in which the open loop frequency response of the system is shaped in such a way that the gain at frequencies before bandwidth is higher to get better tracking and lower at the frequencies after bandwidth to get better precision. While at the same time the phase at the bandwidth should be sufficient to ensure system robustness.

Nevertheless, as suggested by Moore's Law, the size of transistors on ICs is exponentially getting smaller so the industry are always challenged to make the IC smaller and faster as well to maintain productivity. PID suffers fundamental limitations of linear control in which there is a trade off between precision and stability[3]. Because of this, one cannot improve the shape of the gain of open loop frequency response without lowering the value of phase and hence sacrificing stability and robustness. A solution for this is to utilize nonlinear control. However, nonlinear controllers are often too complex and are not accepted by the industry. In reality, the simplicity of controller design and implementation is preferred in industry. Moreover,

loop shaping which enables complete system performance analysis in the frequency domain is preferred as well.

Reset control is one of the nonlinear controllers that is easy to implement. In 1958, Clegg [4] introduced the first reset control by resetting the integrator state when the input crosses zero. This results in less phase lag than a normal integrator while the gain behavior is the same. This is desired since this overcomes the Bode's gain phase relationship which is one of the fundamental limitations of linear control. In addition, loop shaping technique can be employed with reset control by using a pseudo-linearization technique called describing function. Hence, reset control has been applied in several applications [5–15]. Considering the needs of advancement of motion control in the high-tech industry, reset control has the potential to be the new standard. The work in [16] presented the application of reset control for precision applications and shows that reset control can provide significantly improved performance compared to PID. However, the tuning of these newly developed reset controllers still remains unexplored.

Being nonlinear due to resetting action, reset control also introduces higher order harmonics which can cause some unwanted dynamics such as limit cycle. This is not desired in precision systems since this can affect tracking and precision. From this context, the tuning of reset controllers to ensure that we obtain the advantages of the resetting action and avoid the disadvantages of higher order harmonics becomes important. Recently, a new analysis tool known as 'high order sinusoidal input describing function'(HOSIDF) was developed in order to see the frequency behavior of higher order harmonics. It is the extension of describing function which only considers the first harmonic of nonlinear system. HOSIDF allows for a more accurate representation of reset system dynamic [17]. With the information of higher order harmonics, HOSIDF may be useful in the design and tuning of reset systems taking it one step closer towards becoming the next industry standard for controls.

2

LITERATURE REVIEW

This chapter gives the literature review of this thesis which mainly discusses the problem of unwanted dynamics in the reset control application. This chapter is presented in a literature review paper format. In this paper, reset control is first introduced. Secondly, the problem that higher order harmonics create in motion control is addressed. Finally, state of the art of reset strategies developed to handle this problem are reviewed and analysed.

A Review on the Application of Reset Control for Precision Systems

Yusuf Salman
Precision and Microsystem Engineering, TU Delft

***Abstract*—Proportional-Integral-Derivative (PID) controller is the industrial work horse even to this day. However, it has fundamental linear control limitations that inhibit improvement in system performance. Reset control can overcome these limitations while maintaining compatibility with the industry standard loop shaping method. However, it introduces higher order harmonics into the system which might lead to unwanted dynamics such as limit cycles. This phenomenon is a problem in precision systems because it affects tracking and steady-state performance. This paper addresses this issue affecting in reset control systems and discusses the state of the art reset strategies and how they compare from this perspective.**

***Index Terms*—Reset control, Limit cycles, Precision**

I. Introduction

PID is being dominantly used in the precision industry to this day. It can be easily tuned and implemented and also adapts to industry standard loop shaping method and hence allows for broad application. However, there is an increasing demand for higher precision, bandwidth, and robustness from the industry. PID and other linear controllers have fundamental limitations such as the water-bed effect and the Bode's gain-phase relationship [1]. With water-bed effect, improvement of disturbance rejection or noise attenuation in one frequency range results in worsening in another range. As for Bode's gain-phase relationship, the phase is linearly dependent on the slope of gain which inhibits improvement in tracking and precision performance without compromising its stability and robustness.

Nonlinear controllers can overcome these fundamental limitations. Nonetheless, most nonlinear controllers are often complicated. Reset controller is a nonlinear controller where the states are reset when some conditions are satisfied. Apart from its simplicity, reset can be analyzed in the frequency domain using a pseudo-linearization technique called describing function. Hence the loop shaping method can be used with reset control.

The first reset controller was a reset integrator introduced by Clegg in 1958 [2]. Fig. 1 shows reset implementation on an integrator with sinusoidal input. The state of the integrator is reset to zero whenever the input of the integrator crosses zero. The advantage of reset can be shown using describing function in Fig. 2. For reset integrator, the phase lag is 51.9^o less than the linear integrator, but the magnitude is similar. This advantage of reset controller has been now popularly used in many applications, from process control to motion control, as can be found in [3]–[14].

Although reset controllers have reduced phase lag, the resetting action introduces higher order harmonics into the system that lead to unwanted dynamics such as persisting oscillations called limit cycles. This downside of the reset controller affects steady-state precision performance and also tracking performance which is crucial in precision systems. Some works in [6], [15], and [16] have been proposed to cope with the problem.

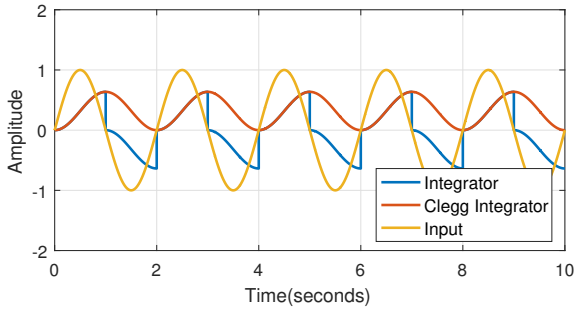

Fig. 1: Integrator and CI output with sinusoid input

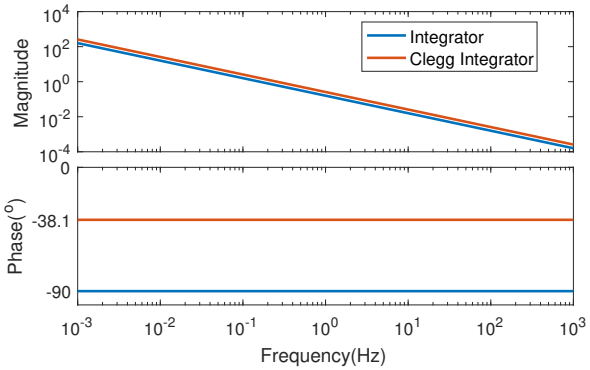

Fig. 2: Frequency response of integrator and CI

This paper provides an overview of reset control along with the problem that comes with its application and the reset strategies that are currently available to overcome this problem. The preliminaries of reset control are provided in Section II. Section III explains the different types of reset elements present in literature. In Section IV, the problem of unwanted limit cycles is discussed along with recent reset strategies developed to deal with it. Section V presents some alternative approaches of reset strategy, followed by conclusions in the last section.

II. Preliminaries

A. Definition

Reset control can be generally defined by Impulsive Differential Equation (IDE) as follows.

$$\Sigma_r := \begin{cases} \dot{\mathbf{x}}_\mathbf{r} = A_r\mathbf{x}_\mathbf{r}(t) + B_r\mathbf{e}(t) & \text{if } (\mathbf{x}_\mathbf{r}(t), \mathbf{e}(t), t_k) \notin \mathcal{M} \\ \mathbf{x}_\mathbf{r}(t^+) = A_\rho\mathbf{x}_\mathbf{r}(t) & \text{if } (\mathbf{x}_\mathbf{r}(t), \mathbf{e}(t), t_k) \in \mathcal{M} \\ \mathbf{u}_\mathbf{r} = C_r\mathbf{x}_\mathbf{r}(t) + D_r\mathbf{e}(t) \end{cases} \quad (1)$$

Where A_r, B_r, C_r, and D_r are the state matrices of the base linear system, $\mathbf{x_r}$ is the state vector, $\mathbf{e}(t)$ and $\mathbf{u_r}(t)$ are the input and the output, respectively. The first and the third equation of (1) represent the base linear system of the controller while the second is the reset mechanism. Reset is triggered when the given condition is satisfied. The after reset value of the states is determined by the resetting matrix A_ρ which is a diagonal matrix. In general, $e(t) = 0$ is the most popularly used condition to determine reset in (1).

B. Describing function analysis

Describing function is a pseudo-linearization method used to approximate the frequency response of the nonlinear reset controller. Only the first harmonic of the output is considered and used to obtain the magnitude and phase. Since zero-crossing reset i.e., resetting when input e(t) crosses zero is the most popular and applied form of reset control, we focus on this type. The describing function of reset element in (1) if the reset condition is $e(t) = 0$ can be obtained as [17] .

$$G(j\omega) = C_r(j\omega I - A_r)^{-1}(I + j\Theta_D(\omega))B_r + D_r \quad (2)$$

where,

$$\Theta_D(\omega) \triangleq -\frac{2\omega^2}{\pi}\Delta(\omega)[\Gamma_D(\omega) - \Lambda^{-1}(\omega)]$$

with,

$$\begin{cases} \Lambda(\omega) \triangleq \omega^2 I + A_r^2 \\ \Delta(\omega) \triangleq I + e^{\frac{\pi}{\omega}A_r} \\ \Delta_D(\omega) \triangleq I + A_\rho e^{\frac{\pi}{\omega}A_r} \\ \Gamma_D(\omega) = \Delta_D^{-1}D\Delta^{-1}(\omega)\Lambda^{-1}(\omega) \end{cases}$$

For other reset systems that do not use reset condition of $e = 0$, the method in [18] can be used to obtain the describing function.

C. Stability of Reset

The stability of the closed loop reset control system which has reset condition of $e(t) = 0$ can be checked by using stability condition given in [1]. The following condition should be checked to ensure asymptotic stability.

Theorem 1: Let $V : \mathbb{R}^n \to \mathbb{R}$ be a continuously differentiable, radially unbounded function, and positive-definite such that

$$\dot{V}(\mathbf{x}) := \left(\frac{\partial V}{\partial \mathbf{x}}\right)^T A_{cl}\mathbf{x} < 0, \quad \text{for} \quad \mathbf{x} \neq 0 \quad (3)$$

$$\delta V(\mathbf{x}) := V(A_R\mathbf{x}) - V(\mathbf{x}) \leq 0, \quad \text{for} \quad \mathbf{x} \in \mathcal{M} \quad (4)$$

Then the reset control system is asymptotically stable.

A_{cl} and A_R are closed loop A-matrix and reset matrix respectively. $\mathbf{x} = \begin{bmatrix} x_R^T & x_p^T \end{bmatrix}^T$ is the state vector. Furthermore, (3) and (4) must satisfy $V(\mathbf{x}) = \mathbf{x}^T P\mathbf{x}$ with $P > 0$ to ensure quadratic stability of the system. Following proposition is used to ensure quadratic stability:

Theorem 2: There exists a constant $\beta \in \mathbb{R}^{n_r \times 1}$ and $P_\rho \in \mathbb{R}^{n_r \times n_r}, P_\rho > 0$ such that the restricted Lyapunov equation.

$$P > 0, \quad A_{cl}^T P + P A_{cl} < 0 \quad (5)$$

$$B_0^T P = C_0 \quad (6)$$

has a solution for P, where C_0 and B_0 are defined by

$$C_0 = \begin{bmatrix} \beta C_p & 0_{n_r \times n_{nr}} & P_\rho \end{bmatrix}, \quad B_0 = \begin{bmatrix} 0_{n_r \times n_r} \\ 0_{n_{nr} \times n_r} \\ I_{n_r \times n_r} \end{bmatrix} \quad (7)$$

where n_r and n_{nr} are the number of reset and non-resetting state of the controller respectively. C_p is $1 \times n_p$ with n_p is the number of plant states.

III. Reset elements

A. Clegg Integrator

Clegg or reset integrator (CI) [2] is the first reset element introduced. It utilizes only an integrator as its base linear system. For CI, the parameters of (1) becomes

$$A_r = 0, \ B_r = 1, \ C_r = 1, \ D_r = 0, \ A_\rho = 0$$

In Fig. 2, describing function of CI shows CI has a phase of -38.1^o compared to a linear integrator which has phase of -90^o. The phase lag of CI can further be controlled by choosing A_ρ to be a non-zero value $\gamma \in [-1, 1]$. This is also known as generalized Clegg integrator (GCI). Fig. 3 shows phase lag obtained with GCI for different values of γ.

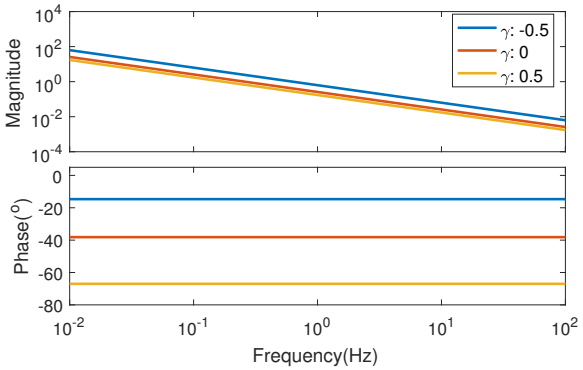

Fig. 3: Generalized CI

B. First Order Reset Element

Horowitz extended CI to a first-order reset element (FORE) that resets the state of a first order low pass filter [19]. The base linear system of FORE is as follows.

$$G(s) = \frac{1}{\frac{s}{\omega_r} + 1} \quad (8)$$

Hence, the parameters of Eq. 1 becomes.

$$A_r = -\omega_r, \quad B_r = \omega_r, \quad C_r = 1, \quad D_r = 0, \quad A_\rho = 0$$

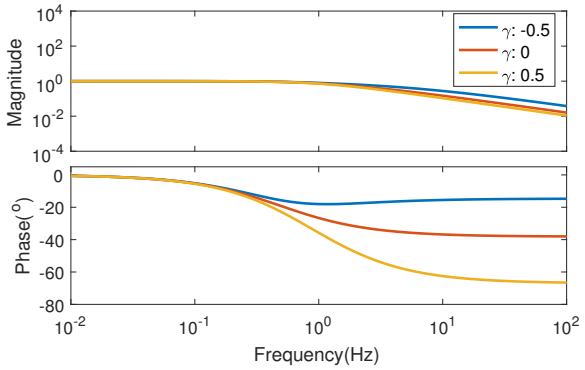

Fig. 4: GFORE

FORE has more design flexibility than CI because of the additional control parameter ω_r. While CI reduces phase lag over entire frequency, FORE behaves similar to its linear counterpart before ω_r and the advantage can mainly be seen after ω_r. Similar to GCI, FORE can also be generalized to Generalized FORE (GFORE) [17]. Fig. 4 shows the describing function of GFORE with different values of γ.

C. Second Order Reset Control

Second-order reset element (SORE) resets a second-order element such as second-order low-pass filter or notch filter [10]. Consider a base linear system as given below.

$$G(s) = \frac{\omega_r^2}{s^2 + 2\beta_r\omega_r s + \omega_r^2} \tag{9}$$

The parameters of 1 are obtained as.

$$A_r = \begin{bmatrix} 0 & 1 \\ -\omega_r^2 & -2\beta_r\omega_r \end{bmatrix} \qquad B_r = \begin{bmatrix} 0 \\ \omega_r^2 \end{bmatrix}$$

$$C_r = \begin{bmatrix} 1 & 0 \end{bmatrix} \qquad A_\rho = \begin{bmatrix} 0_{n_r \times n_r} \end{bmatrix}$$

SORE gives more degree of freedom to design a reset element compared to FORE with the addition of damping ratio β_r. Different from the damping ratio of linear second-order element (when $A_\rho = 1$), change in β_r of SORE affects change in phase behavior with very little effect on gain behavior. To show this is the case, the frequency response of SORE for different values of β_r is shown in Fig. 5. It can be seen that adjusting β_r allows for shaping of the phase behavior with minimal effect on gain.

SORE can be generalized with the relaxation of default reset matrix A_ρ. The Generalized SORE (GSORE) takes A_ρ to the following form.

$$A_\rho = \gamma \begin{bmatrix} 1 & 0 \\ 0 & 1 \end{bmatrix}$$

D. Generalization of reset controller

The reset element of first and second order has been presented in the previous subsection. It is seen that generalization of these reset elements are mainly made by relaxing the after reset value matrix A_ρ. Furthermore, a reset controller of any n^{th} order element of Eq.1 can be generalized such that A_ρ is in the following form [20].

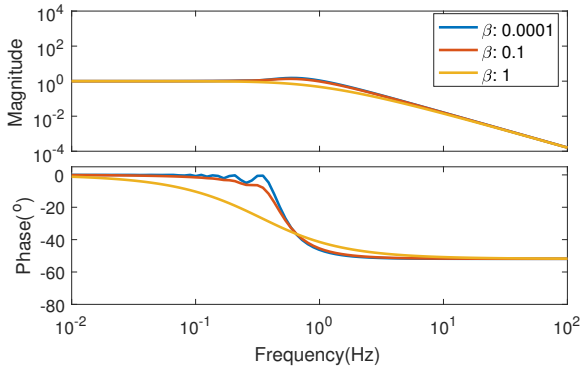

Fig. 5: SORE with different β_r

$$A_\rho = \begin{bmatrix} \gamma_1 & 0 & \dots & 0 & 0 \\ 0 & \gamma_2 & \dots & 0 & 0 \\ 0 & 0 & \dots & \gamma_{n_r} & 0 \\ 0 & 0 & \dots & 0 & I_{n_{nr} \times n_{nr}} \end{bmatrix}$$

In which n_r and n_{nr} are, respectively, number of resetting and non-resetting states of overall controller with $n_r + n_{nr} = n$. By this form of generalization, one can vary the behavior of reset control by adjusting the value of γ_i $(i = 1 \dots n_r)$.

IV. Limit Cycles and Loss of Precision with Reset

A. Limit cycles in reset control system

Reset control provides better performance than linear control by overcoming the limitation of linear controller [1], but on the other hand unwanted dynamics may occur due to the nonlinearity of reset [21]. To show that is the case, consider a closed loop system in Fig. 6

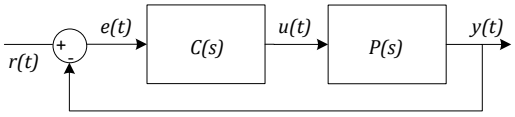

Fig. 6: Closed loop system

where the plant is given as follows

$$P(s) = \frac{1}{s+1} \tag{10}$$

and the controller is a PI controller, $C(s)$ is given below.

$$C(s) := \begin{cases} \dot{x}(t) = e(t) \\ u(t) = 0.5x(t) + 5e(t) \end{cases} \tag{11}$$

A P-Clegg integrator (PCI) can be designed by introducing reset into this PI controller such that the after reset equation is provided as $x(t) = 0$ every time $e(t)$ crosses zero. Fig. 7 shows the open loop frequency response of the system in Fig. 6 controlled by PI and PCI.

It can be seen that higher phase is obtained by PCI controller compared to PI controller at bandwidth frequency ω_c. As a result, the system with PCI results in less overshoot in step response since its phase margin is higher, as shown in Fig. 8. However, there is a persistent oscillation near the set-point for the PCI system so that the steady-state condition is not achieved. This persisting oscillation is what referred as limit cycles.

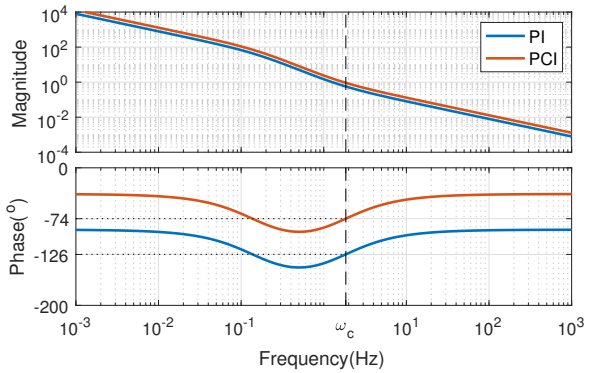

Fig. 7: Frequency responses of closed loop system controlled by PI and PCI

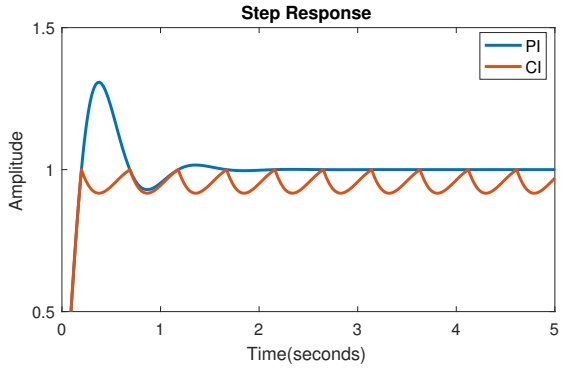

Fig. 8: Loss of precision due to limit cycles

Some reset control design strategies have been developed to handle this since this can affect overall performance of the system. In this section, a brief overview of these state of the art reset control strategies is given and discussed.

B. Reset strategies

1) PI+CI: PI+CI controller combines a proportional gain, a linear integrator and a CI in parallel. The structure of the controller is shown by Fig. 9. The configuration remains simple for tuning since p_r is the only additional parameter. $p_r \in [0, 1]$ determines the weight of linear integrator over the CI. This reset strategy reduces the limit cycle while at the same time reducing phase lag compared to a linear controller. This is done because the linear integrator compensates for the steady state error while CI provides phase lag reduction.

To illustrate how PI+CI performs, consider a system in Fig. 6 with the plant of Eq. 10 controlled by PI+CI controller with $k_p = 5$ and $\tau_i = 0.1$. The step response of the system for different values of p_r is shown in Fig. 10. It can be seen that limit cycle is reduced as the value of p_r decreases. For lesser

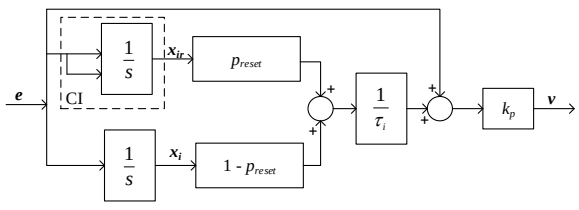

Fig. 9: PI+CI structure

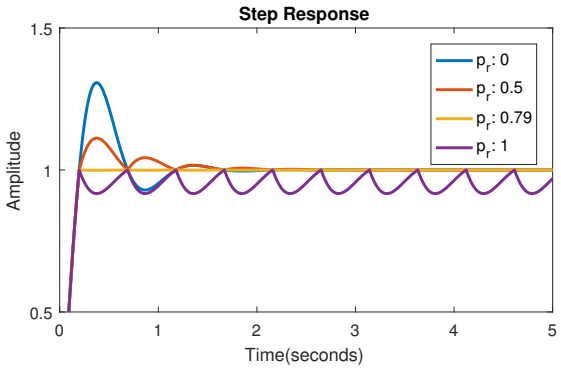

Fig. 10: PI+CI with different p_r

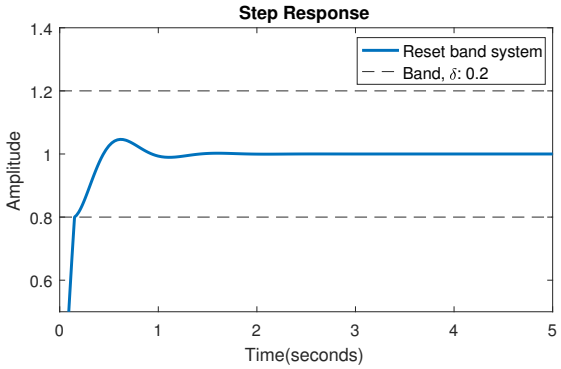

Fig. 11: Reset band system achieves steady state condition

values of p_r, more overshoot is seen since phase lag reduction is less.

One can see that by adjusting p_r, the controller becomes more like PI or PCI, and as a result, p_r is the parameter to determine the nonlinearity of reset control. In other words, the PI+CI controller only provides a trade-off between PI and PCI. This translates to a trade-off between robustness and limit cycles such that this strategy does not use the full advantage of reset control. It must be noted that PI+CI approach provides a similar trade-off that value of γ in A_ρ provides.

2) Reset with band: Reset with band is a type of reset control in which reset action is applied when input enters a reset band. Reset control with band is expressed by the following equation.

$$\begin{cases} \dot{\mathbf{x}}_\mathbf{r} = A_r \mathbf{x}_\mathbf{r}(t) + B_r \mathbf{e}(t) & \text{if } (\mathbf{e}(t), \dot{\mathbf{e}}(t)) \notin B_\delta \\ \mathbf{x}_\mathbf{r}(t^+) = A_\rho \mathbf{x}_\mathbf{r}(t) & \text{if } (\mathbf{e}(t), \dot{\mathbf{e}}(t)) \in B_\delta \\ \mathbf{u}_\mathbf{r} = C_r \mathbf{x}_\mathbf{r}(t) + D_r \mathbf{e}(t) \end{cases} \tag{12}$$

where,

$$B_\delta = (x, y) \in (R)^2 | (x = -\delta \wedge y > 0) \vee (x = \delta \wedge y < 0)$$

and δ is a non-negative real number that determines the region of reset band.

The use of band compensates more phase than that of zero crossing reset condition, hence reset band controller has more robustness, and improves performance, especially for systems with delay [16]. To see how reset band reduces limit cycle, let a system as shown in Fig. 6 have plant of $P(s) = \frac{1}{s+1}$ and controller of Eq. 12 with $[A_r, B_r, C_r, D_r] = [0, 1, 0.5, 5]$ and $\delta = 0.2$. In Fig. 11, the limit cycle does not appear in the step response of the system.

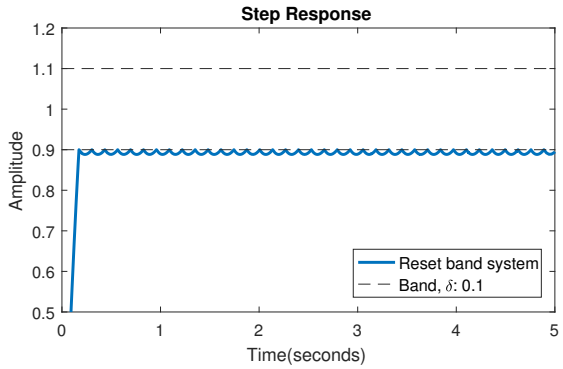

Fig. 12: Reset band system suffers limit cycle

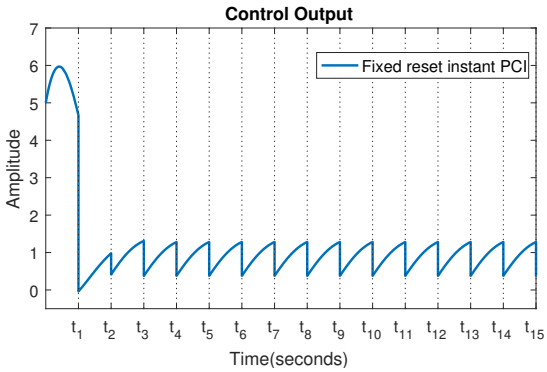

Fig. 13: Fixed reset time instant reset controller resets regardless the controller input

This reduction of limit cycles, however, depends on the value of band δ. For instance, with a different value of δ, the same system suffers limit cycles around its band line, see Fig. 12. Thus, reset band controller is not a robust solution for a practical system with model uncertainties. Besides, there is no literature which provides the specific procedure to determine the reset band.

3) Fixed reset instant: In fixed reset instant strategy, reset action is executed at pre-specified fixed time instant, $t_k, (k = 1, ..)$, see Fig. 13.

Guo et. al. [6] developed a reset control that incorporates fixed reset instant with the addition of non-zero after reset value. In [6], the limit cycles are almost reduced since the after reset state is set based on tracking error minimization. While the time instant parameter is presented as trivial in [6], the overall system performance is significantly determined by these reset instants. Nonetheless, in [6], t_k value is defined arbitrarily and the after reset values $x_r(t_k^+)$ is determined based on system model and the determined t_k. Consequently, this reset strategy is not robust to model uncertainties and besides there is no procedure to determine Δt_k.

4) Feedforward controller: Based on the final value theorem analysis in [22], a closed loop system in Fig. 14 with a plant of $P(s)$ and feedback controller of $R(s)$ and feedforward controller of $FF(s)$ can achieve a steady-state condition if the value of $FF(s)$ is chosen to be inverse of $P(s)$. Note that in the case of limit cycles, the steady-state condition is not achieved. Therefore, a feedforward controller can be added to avoid limit cycles. Zaccarian et. al. [23] has shown the use of feedforward, as a set-point regulator, enables the system to

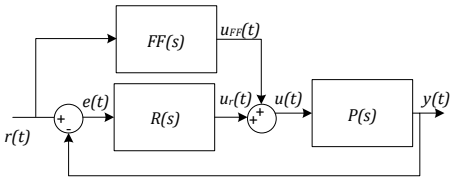

Fig. 14: Reset controller $R(s)$ with feedforward $FF(s)$

avoid limit cycles.

However, in the event of external disturbances or model uncertainty, the feedforward controller is not able to maintain the steady-state condition. Reset strategies such as adaptive feedforward [24], [25] and iterative learning control (ILC) [26] were proposed as modification of basic feedforward controller in order to adapt system uncertainty. While these approaches are promising, adaptive techniques require time to adapt and fail in case of sporadic disturbances and iterative learning strategies require repetitive trajectories and disturbances.

V. Alternative Approaches with Reset

Most of the work in reset control has focussed on the phase lag reduction advantage seen with reset. More importantly, most of the work has also only focussed on the integrator. However recent works in [8], [27]–[29], show the use of reset in other parts of the controller with the idea of using reset for phase compensation rather than phase lag reduction. Li et. al. [8] used reset control in a narrow-band filter to compensate for the phase lag seen with the use of an anti-notch filter. The result is a robust disturbance compensator in a narrow band.

Works in [28] and [29] employ reset control to design a new controller within fractional and integer order of PID framework. As a result, more improvement in performance than PID is achieved. A PID transfer function is given as follows.

$$C(s) = k_p \underbrace{(1 + \frac{\omega_i}{s})}_{\text{Integrator}} \underbrace{\frac{(1 + \frac{s}{\omega_d})}{(1 + \frac{s}{\omega_t})}}_{\text{Tamed derivative}} \underbrace{\frac{1}{1 + \frac{s}{\omega_f}}}_{\text{Low pass}} \tag{13}$$

Where ω_i, ω_d, ω_t, and ω_f are the cut-off frequency of integrator, lead, lag and low pass element of PID, respectively.

Instead of purely focusing on resetting the integrator as is done in prior work, research in [29] looked at introduction of reset in different parts of PID for improved performance.

Similarly in [28], Chen et. al. introduced reset mechanism into the framework of fractional order controllers obtained through CRONE methodology. Reset applied to different parts of the controller was explored. From the results of [28] and [29], it is seen that the higher order harmonics deteriorate overall performance mainly when reset is used in the integrator part.

While the use of good feedforward helped in [28] and [29], these works provided robust solutions for using reset with significantly reduced effect of the higher order harmonics compared to the other techniques presented in Section IV. The work in [29] was extended in [20] in the form of a novel reset element termed 'Constant in gain Lead in phase (CgLp)' which uses a linear lead with a GFORE element. This element was used with PID to provide broadband phase compensation

and was shown to improve performance significantly. However it was also seen that the improvement seen was dependent on the tuning of this reset element and PID. Unfortunately, no literature exists currently for the tuning of these reset elements.

VI. Conclusion

Reset control is gaining popularity because it outperforms PID. However, the nonlinearity of reset control introduces higher order harmonics to the system such that unwanted dynamics like limit cycles may be present in the system response. The unwanted dynamics problem in reset control is crucial in precision systems because it affects tracking and precision.

PI+CI, reset band, fixed reset instants and feedforward are the strategies that can be used to avoid or reduce limit cycles. Nevertheless, these strategies have significant drawbacks and are not robust. PI+CI is actually a trade-off between linear and nonlinear control, so it does not use complete potential of reset control. Whereas reset band, fixed reset instant, and feedforward are less robust against model uncertainties, since the value of band δ, reset time instant t_k and feedforward depends on system characteristics.

While most literature has focused on implementing reset in integrator. Some works have implemented reset in other parts of linear controller. From the result of these works, it is observed that this results in less undesired response. This technique of using reset in a different part of the controller for phase compensation rather than phase lag reduction is more robust and provides a good path for future research.

One main problem with study of reset systems is that describing function is used for frequency domain analysis. Since this is an approximation, unwanted dynamics like limit cycles cannot be seen in the frequency domain. Hence, more advanced tools for more accurate representation needs to be developed and used to ensure that reset control can replace linear PID as the next industrial machine.

References

[1] A. Banos, J. Carrasco, and A. Barreiro, "Reset Times-Dependent Stability of Reset Control Systems," *IEEE Transactions on Automatic Control*, vol. 56, no. 1, pp. 217–223, 2011. [Online]. Available: http://ieeexplore.ieee.org/document/5605653/

[2] J. C. Clegg, "A nonlinear integrator for servomechanisms," *Transactions of the American Institute of Electrical Engineers, Part II: Applications and Industry*, vol. 77, no. 1, pp. 41–42, 1958. [Online]. Available: http://ieeexplore.ieee.org/document/6367399/

[3] J. Moreno, J. Guzmán, J. Normey-Rico, A. Baños, and M. Berenguel, "A combined FSP and reset control approach to improve the set-point tracking task of dead-time processes," *Control Engineering Practice*, vol. 21, no. 4, pp. 351–359, 4 2013. [Online]. Available: https://www.sciencedirect.com/science/article/pii/S0967066112002560

[4] M. A. Davo and A. Banos, "Reset control of a liquid level process," in *2013 IEEE 18th Conference on Emerging Technologies & Factory Automation (ETFA)*. IEEE, 9 2013, pp. 1–4. [Online]. Available: http://ieeexplore.ieee.org/document/6648111/

[5] F. Perez, A. Banos, and J. Cervera, "Periodic reset control of an in-line pH process," in *ETFA2011*. IEEE, 9 2011, pp. 1–4. [Online]. Available: http://ieeexplore.ieee.org/document/6059208/

[6] Y. Guo, J. Zheng, M. Fu, Y. Wang, and L. Xie, "Development of an extended reset controller and its experimental demonstration," *IET Control Theory & Applications*, vol. 2, no. 10, pp. 866–874, 2008.

[7] M. Heertjes, K. Gruntjens, S. van Loon, N. Kontaras, and W. Heemels, "Design of a variable gain integrator with reset," in *2015 American Control Conference (ACC)*. IEEE, 7 2015, pp. 2155–2160. [Online]. Available: http://ieeexplore.ieee.org/document/7171052/

[8] Y. Li, G. Guo, and Y. Wang, "Reset Control for Midfrequency Narrowband Disturbance Rejection With an Application in Hard Disk Drives," *IEEE Transactions on Control Systems Technology*, vol. 19, no. 6, pp. 1339–1348, 11 2011. [Online]. Available: http://ieeexplore.ieee.org/document/5639061/

[9] Y. Li, X. Guo, and Y. Wang, "Phase lead reset control design with an application to HDD servo systems," in *9th International Conference on Control, Automation, Robotics and Vision, 2006, ICARCV '06*, 2006.

[10] L. Hazeleger, M. Heertjes, and H. Nijmeijer, "Second-order reset elements for stage control design," in *2016 American Control Conference (ACC)*. IEEE, 7 2016, pp. 2643–2648. [Online]. Available: http://ieeexplore.ieee.org/document/7525315/

[11] Y. Zheng, Y. Chait, C. Hollot, M. Steinbuch, and M. Norg, "Experimental demonstration of reset control design," *Control Engineering Practice*, vol. 8, no. 2, pp. 113–120, 2 2000. [Online]. Available: https://www.sciencedirect.com/science/article/pii/S0967066199001318

[12] E. Delgado, M. Diaz-Cacho, A. Banos, and A. Barreiro, "Reset control of synchronous motors with permanent magnet excitation," in *22nd Mediterranean Conference on Control and Automation*. IEEE, 6 2014, pp. 1347–1352. [Online]. Available: http://ieeexplore.ieee.org/document/6961563/

[13] E. Delgado, A. Barreiro, M. Diaz-Cacho, and P. Falcon, "Wheel slip reset controller in automotive brake systems," in *2014 IEEE International Electric Vehicle Conference (IEVC)*. IEEE, 12 2014, pp. 1–6. [Online]. Available: http://ieeexplore.ieee.org/document/7056103/

[14] A. Costas, M. Cerdeira-Corujo, A. Barreiro, E. Delgado, and A. Banos, "Car platooning reconfiguration applying reset control techniques," in *2016 IEEE 21st International Conference on Emerging Technologies and Factory Automation (ETFA)*. IEEE, 9 2016, pp. 1–8. [Online]. Available: http://ieeexplore.ieee.org/document/7733592/

[15] A. Baños and A. Vidal, "Definition and tuning of a PI+ CI reset controller," *Control Conference (ECC), 2007 European*, pp. 4792–4798, 2007.

[16] A. Baños, S. Dormido, and A. Barreiro, "Limit cycles analysis of reset control systems with reset band," *IFAC Proceedings Volumes (IFAC-PapersOnline)*, vol. 3, no. PART 1, pp. 180–185, 2009. [Online]. Available: http://dx.doi.org/10.1016/j.nahs.2010.07.004

[17] Y. Guo, Y. Wang, and L. Xie, "Frequency-domain properties of reset systems with application in hard-disk-drive systems," *IEEE Transactions on Control Systems Technology*, vol. 17, no. 6, pp. 1446–1453, 2009.

[18] C. Schwartz and R. Gran, "Describing function analysis using MATLAB and Simulink," *IEEE Control Systems Magazine*, vol. 21, no. 4, pp. 19–26, 2001. [Online]. Available: http://ieeexplore.ieee.org/document/939940/

[19] I. Horowitz and P. Rosenbaum, "Non-linear design for cost of feedback reduction in systems with large parameter uncertainty," *International Journal of Control*, vol. 21, no. 6, pp. 977–1001, 6 1975. [Online]. Available: http://www.tandfonline.com/doi/abs/10.1080/00207177508922051

[20] N. Saikumar, R. K. Sinha, and S. H. Hosseinnia, " Constant in gain Lead in phase element - Application in precision motion control," no. 1, pp. 1–9.

[21] M. Ivens, "Robust Reset Control using Adaptive / Iterative Learning Control," 2018. [Online]. Available: https://repository.tudelft.nl/islandora/object/uuid:736ac020-25f8-4e03-8a3e-46569e79974b?collection=education

[22] L. Chen, "Development of CRONE reset control," Ph.D. dissertation, TU Delft, 2017. [Online]. Available: https://repository.tudelft.nl/islandora/object/uuid:5370c610-4112-49e9-b860-9d625d5b40c5?collection=education

[23] L. Zaccarian, D. Nesic, and A. R. Teel, "Set-point stabilization of SISO linear systems using First Order Reset Elements," in *2007 American Control Conference*. IEEE, 7 2007, pp. 5808–5809. [Online]. Available: http://ieeexplore.ieee.org/document/4282505/

[24] F. S. Panni, H. Waschl, D. Alberer, and L. Zaccarian, "Position Regulation of an EGR Valve Using Reset Control With Adaptive Feedforward," *IEEE Transactions on Control Systems Technology*, vol. 22, no. 6, pp. 2424–2431, 11 2014. [Online]. Available: http://ieeexplore.ieee.org/document/6778034/

[25] M. Cordioli, M. Mueller, F. Panizzolo, F. Biral, and L. Zaccarian, "An adaptive reset control scheme for valve current tracking in a power-split transmission system," in *2015 European Control Conference (ECC)*. IEEE, 7 2015, pp. 1884–1889. [Online]. Available: http://ieeexplore.ieee.org/document/7330813/

[26] S. H. HosseinNia, I. Tejado, B. M. Vinagre, and Y. Chen, "Iterative Learning and Fractional Reset Control," in *Volume 9: 2015 ASME/IEEE International Conference on Mechatronic and Embedded Systems and Applications*. ASME, 8 2015, p. V009T07A041.

[27] H. Li, C. Du, and Y. Wang, "Optimal Reset Control for a Dual-Stage Actuator System in HDDs," *IEEE/ASME Transactions on Mechatronics*, vol. 16, no. 3, pp. 480–488, 6 2011. [Online]. Available: http://ieeexplore.ieee.org/document/5752858/

[28] L. Chen, N. Saikumar, S. Baldi, and S. H. HosseinNia, "Beyond the Waterbed Effect: Development of Fractional Order CRONE Control with Non-Linear Reset," 5 2018. [Online]. Available: http://arxiv.org/abs/1805.10037

[29] A. Palanikumar, N. Saikumar, and S. H. HosseinNia, "No More Differentiator in PID:Development of Nonlinear Lead for Precision Mechatronics," 5 2018. [Online]. Available: http://arxiv.org/abs/1805.09703

3

OBJECTIVE

3.1. PROBLEM DEFINITION

In order to make reset control more reliable for the high-tech precision industry, there is a need to find robust solutions so that the full potential of reset control can be utilized while reducing higher order harmonics and their effects and also ensuring simplicity of controller in both design and implementation. A review of existing strategies towards this goal shows that most techniques are not robust. However, the phase compensation techniques show some promising results towards this end.

The controller designed in [16] using the novel reset element termed 'Constant in Gain, Lead in Phase' (CgLp) shows the potential of reset control. The controller presented in [16] surpasses PID performance but is still compatible with the PID loop shaping technique with the use of only a basic reset element. However tuning of the reset element is critical to obtain good performance.

Optimal tuning of reset elements including CgLp is only possible in frequency domain if the higher order harmonics are also considered during tuning. Recently, a tool termed Higher order sinusoidal input describing function was developed to visualize these harmonics. A study on higher order harmonics using HOSIDF may help understand the harmonics effect on closed loop system behavior. Thus this research will focus on the study of CgLp using describing function and HOSIDF and the development of tuning rules for reset control based on these tools. The way this tuning problem is formulated is given in Appendix A.

3.2. RESEARCH GOAL AND QUESTION

This thesis' reseach goal is *to obtain tuning rules for reset controllers through analysis with describing function and HOSIDF*. In order to reach this goal, following research questions have to be answered:

1. What is the effect of the different controller parameter values on the higher order harmonics?
2. How do these higher order harmonics affect tracking and precision performance?
3. How should a reset controller with CgLp be designed and tuned?

3.3. THESIS OUTLINE

Chapter 1 has introduced the motivation of this research. In the second chapter, the literature review of this thesis is given. This section provides the formulation of the problem along with the objective of this thesis. The main contribution of this thesis, a study on reset control through describing function and HOSIDF is provided in scientific paper format in Chapter 4. Finally, Chapter 5 presents the conclusion and recommendation for the future research.

More details on this research are in the appendices. Appendix A presents the optimization problem of tuning CgLp. Appendix B provides brief explanation on the experiment setup. Appendix C provides the complete frequency response plot of the open loop system in Chapter 4. Appendix D gives the code used for implementation that consists of MATLAB and Simulink Code.

4

TUNING OF 'CONSTANT-GAIN LEAD-PHASE' WITH DESCRIBING FUNCTION AND HOSIDF

This chapter is presented in scientific paper format. It describes the tuning of the novel reset element Constant-Gain Lead-Phase (CgLp) in PID framework using describing function and HOSIDF. The first part of the work concentrates on the analysis of CgLp performance indices obtained on a practical setup using the describing function and HOSIDF rules. Then, this analysis is used to obtain some basic guidelines for the tuning of CgLp.

Tuning of 'Constant in gain Lead in Phase' element for Precision Motion Systems

Yusuf Salman, Niranjan Saikumar, and Hassan HosseinNia
Precision and Microsystem Engineering,
Faculty of Mechanical, Maritime and Materials Engineering, TU Delft, The Netherlands

***Abstract*—This paper presents tuning guidelines for 'Constant in gain and Lead in Phase' (CgLp) controller based on the study of its first and higher order harmonics. CgLp is a novel reset element developed to overcome the fundamental limitations of Proportional-Integral-Derivative (PID) control. Despite its merit, the nonlinearity of reset action in CgLp results in the presence of higher order harmonics. Until recently, describing function analysis has been commonly used to analyze reset systems while the higher order harmonics have been neglected. In this paper, these harmonics are studied through higher order sinusoidal input describing function (HOSIDF) and their effect on system performance (tracking and precision) is studied experimentally. This is used to obtain some basic tuning guidelines for designing controllers using CgLp.**

***Index Terms*—Reset control, precision control, motion control, describing function, HOSIDF**

I. Introduction

PID has been the industry standard for several decades [1]. It has a wide application from the process industry to high-tech industry due to its simplicity in design and implementation. Loop shaping technique can be used to design and analyze complete system performance in the frequency domain. Combined with good feedforward control, PID can provide high bandwidths, precision, good tracking and robustness. Their performance and reliability has ensured that it is the go-to controller used in precision applications such as wafer scanners, atomic force microscopes etc.

However, PID cannot meet the increasing demands of the high-tech industry where faster, more precise and more robust control is expected. As a linear controller, PID has fundamental limitations of Bode's gain phase relationship and waterbed effect [2]. It is required for the frequency response of open loop transfer function to have high gain at frequencies before bandwidth in order to obtain good tracking performance, lower gain at high frequencies to have better noise attenuation, and sufficient phase at bandwidth (phase margin) to ensure system robustness and stability. Integrator increases the gain at low frequency, low pass filter makes the gain at high frequency lower, and differentiator supplies phase for phase margin. The more phase added by differentiator results in reducing the gain at low frequencies and increasing it at high frequencies. This is due to Bode's gain phase relationship. These limitations can only be overcome by making use of nonlinear control.

Reset control is a nonlinear-type controller which has gained popularity in recent years. In 1958, Clegg [3] introduced the first reset control and showed that resetting the state of an integrator when the input crosses zero results in 52.1^o less phase lag compared to a linear integrator, see Fig.1. In that case, with the addition of only reset mechanism to the linear system, the limitation of the linear controller is overcome. Using describing function analysis as an approximation technique to obtain frequency domain behaviour, loop shaping can be used to design reset control ensuring the compatibility with industry. Further, since reset control is achieved by resetting one of the states of a base linear system, it also makes it compatible with the PID framework also popular with the industry. Since Clegg, other reset elements namely First Order Reset Element (FORE) [4], Generalized FORE [5], Second Order Reset Element (SORE) [6], and Generalized SORE [7] have been introduced providing more freedom in the design and utilization of reset control. Some works have shown the use of reset control in precision motion systems, as can be found in [5], [8]–[11]. While reset control has mainly been used for its phase lag reduction, some works exist where reset has been used for phase compensation as well [11]–[13]. For instance, in [11], a reset element is used to compensate the phase loss caused by the use of a notch filter in a narrowband. As a result, disturbance rejection near bandwidth is made possible without decreasing the phase margin.

Saikumar et. al. [7] introduced a new reset element termed 'Constant in gain and Lead in phase' (CgLp). This work allows for phase compensation in a broadband frequency range. They show the integration of CgLp with PID improves the performance of a precision motion system in bandwidth, tracking and steady state precision without lowering the phase margin. Another example of the utilization of CgLp can be found in [14]. However, no information is provided on the

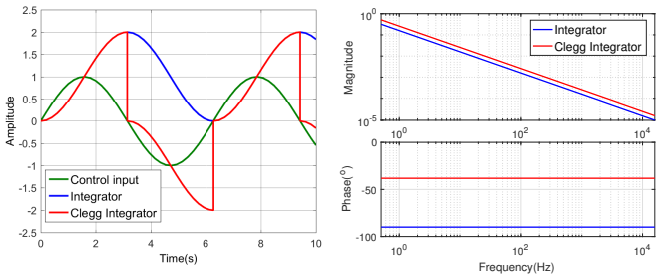

(a) (b)

Fig. 1: Integrator and reset integrator in (a) time domain, and its (b) frequency response

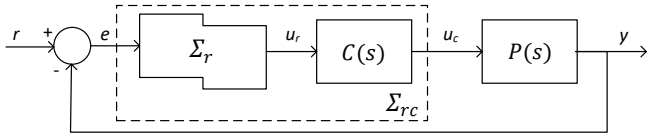

Fig. 2: Reset control closed loop system

required tuning of this CgLp element. In fact, it was seen that in some cases, the improvement expected through describing function analysis was not seen and in the worst case scenario, deterioration in performance was also noticed. As a nonlinear element, CgLp introduces higher order harmonics into the system which can negatively affect system performance. Hence, describing function as a tool to do frequency analysis for the reset control is insufficient since it only considers first harmonic. Recently, Heinen [15] extended describing function into high order sinusoidal describing function (HOSIDF). With this analysis tool, more accurate frequency analysis of reset control can be performed since higher order harmonics can be visualised and considered during analysis.

This paper aims to perform a performance analysis for CgLp element by taking the first and higher order harmonics into account using describing function and HOSIDF. From the knowledge obtained, a design guideline to tune a CgLp in open loop based on HOSIDF can be obtained. Preliminaries of reset control are first provided in Section II. In Section III, Cglp element is explained along with the procedure to design a controller with CgLp and PID. Section IV presents the performance analysis of the so-called CgLp-PID which is implemented on a precision motion system to obtain closed loop tracking and precision performance. In the same section, a design guideline for CgLp is established. Finally, the conclusion is provided in Section V.

II. Preliminaries

A. Definition of reset control

A general reset control can be defined by the following differential equations:

$$\Sigma_r := \begin{cases} \dot{x}_r & = A_r x_r(t) + B_r e(t) & \text{if } e \neq 0 \\ x_r(t^+) & = A_\rho x_r(t) & \text{if } e = 0 \\ u_r & = C_r x_r(t) + D_r e(t) & \end{cases} \tag{1}$$

where A_r, B_r, C_r, and D_r are the base linear system state matrices, $\mathbf{x_r}$ is the state vector, $e(t)$ and $u_r(t)$ are error input and control output, respectively. A_ρ is the reset matrix that determines the after-reset values of the states. The first and the third equation of (1) represent the base linear system of the controller while the second is the reset mechanism. $A_\rho = I$ means no reset action is done and the controller acts as a regular linear controller, and A_ρ equals to zero matrix results in traditional reset where all the states are reset to zero. If $A_\rho = \gamma I$, where $\gamma \in [0, 1]$, then partial reset is achieved This reset control in series with linear controller $C(s)$ is implemented in a closed-loop control to control a plant $P(s)$ depicted in Fig. 2

B. Describing function analysis

Describing function is a pseudo-linear approximation of frequency response of a nonlinear system. It considers only the first harmonic of the open loop response of the nonlinear system. Although this is an approximation technique, this has been popularly used in literature for design and analysis. The describing function of reset control of equation (1) is as follows [5].

$$\Sigma_r(\omega) = C_r(j\omega I - A_r)^{-1}(I + j\Theta_D(\omega))B_r + D_r \tag{2}$$

where,

$$\Theta_D(\omega) \triangleq -\frac{2\omega^2}{\pi}\Delta(\omega)[\Gamma_D(\omega) - \Lambda^{-1}(\omega)]$$

with the parameters used as follows,

$$\begin{cases} \Lambda(\omega) & \triangleq & \omega^2 I + A_r^2 \\ \Delta(\omega) & \triangleq & I + e^{\frac{\pi}{\omega}A_r} \\ \Delta_D(\omega) & \triangleq & I + A_\rho e^{\frac{\pi}{\omega}A_r} \\ \Gamma_D(\omega) & = & \Delta_D^{-1} D \Delta^{-1}(\omega)\Lambda^{-1}(\omega) \end{cases}$$

C. Higher order sinusoid describing function (HOSIDF)

Although reset controllers have been designed in literature through describing function, Heinen [15] pointed out the various inaccuracies of this method especially for analysis of closed loop performance including overall stability. Hence, Heinen also developed HOSIDF to visualise high order harmonics which also affect system performance. Following is the HOSIDF equation derived analytically for the reset controller in (1) [15].

$$\Sigma_{r(n)}(\omega, n) = \begin{cases} C^T(j\omega n I - A)^{-1} j\Theta_D(\omega) B & \text{for odd } n \geq 2 \\ 0 & \text{for even } n \geq 2 \end{cases} \tag{3}$$

where n is the order of harmonic. The higher order harmonics of open loop system in Fig. 2 is calculated as follows [15].

$$L_n(\omega, n) = \Sigma_{r(n)}(\omega, n) C(j\omega n) P(j\omega n) \tag{4}$$

D. Stability analysis of reset control system

The stability of the closed loop reset control system as shown in Fig. 2 which has reset condition of $e(t) = 0$ can be checked by using stability condition given in [2]. The following condition should be checked to ensure asymptotic stability.

Theorem 1: Let $V : \mathbb{R}^n \to \mathbb{R}$ be a continuously differentiable, radially unbounded function, and positive-definite such that

$$\dot{V}(\mathbf{x}) := \left(\frac{\partial V}{\partial \mathbf{x}}\right)^T A_{cl}\mathbf{x} < 0, \quad \text{for} \quad \mathbf{x} \neq 0 \tag{5}$$

$$\delta V(\mathbf{x}) := V(A_R\mathbf{x}) - V(\mathbf{x}) \leq 0, \quad \text{for} \quad \mathbf{x} \in \mathcal{M} \tag{6}$$

Then the reset control system is asymptotically stable.
A_{cl} and A_R are closed loop A-matrix and reset matrix respectively. $\mathbf{x} = \begin{bmatrix} x_R^T & x_p^T \end{bmatrix}^T$ is the state vector. Furthermore, (5) and (6) must satisfy $V(\mathbf{x}) = \mathbf{x}^T P \mathbf{x}$ with $P > 0$ to ensure quadratic stability of the system. Following proposition is used to ensure quadratic stability:

Theorem 2: There exists a constant $\beta \in \mathbb{R}^{n_r \times 1}$ and $P_\rho \in \mathbb{R}^{n_r \times n_r}, P_\rho > 0$ such that the restricted Lyapunov equation.

$$P > 0, \quad A_{cl}^T P + P A_{cl} < 0 \tag{7}$$

$$B_0^T P = C_0 \tag{8}$$

has a solution for P, where C_0 and B_0 are defined by

$$C_0 = \begin{bmatrix} \beta C_p & 0_{n_r \times n_{nr}} & P_\rho \end{bmatrix}, \quad B_0 = \begin{bmatrix} 0_{n_r \times n_r} \\ 0_{n_{nr} \times n_r} \\ I_{n_r \times n_r} \end{bmatrix} \tag{9}$$

where n_r and n_{nr} are the number of reset and non-resetting state of the controller respectively. C_p is $1 \times n_p$ with n_p is the number of plant states.

III. Constant-gain Lead-phase (CgLp)

A. CgLp introduction

CgLp was introduced by Saikumar et. al. [7] as a reset element formed by the combination of a GFORE (resetting first order lag filter) with a first-order lead filter, which are both denoted respectively as R and F in (10).

$$R = \frac{1}{\left(\frac{s}{\omega_{r\alpha}} + 1\right)^{\gamma}} \quad \text{and} \quad F = \frac{\frac{s}{\omega_r} + 1}{\frac{s}{\omega_f} + 1} \tag{10}$$

Where $\omega_f >> \omega_{r\alpha}, \omega_r$. The matrices of CgLp for (1) are as follows

$$A_r = \begin{bmatrix} -\omega_{r\alpha} & 0 \\ \omega_f & -\omega_f \end{bmatrix}, \quad B_r = \begin{bmatrix} \omega_{r\alpha} \\ 0 \end{bmatrix}$$

$$C_r = \begin{bmatrix} \frac{\omega_f}{\omega_r} & \left(1 - \frac{\omega_f}{\omega_r}\right) \end{bmatrix}, \quad D_r = \begin{bmatrix} 0 \end{bmatrix}$$

$$A_\rho = \begin{bmatrix} \gamma & 0 \\ 0 & 1 \end{bmatrix}$$

Since the resetting action does not influence the magnitude behaviour of the filter significantly, this combination of reset lag with linear lead results in no change in gain. However, phase lead is obtained over a wide range starting from ω_r until ω_f. Further, as γ is varied, the amount of phase lead achieved can also be controlled as shown in Fig. 3. Although the magnitude behaviour of GFORE is not affected significantly compared to linear first order filter, this small change was found to be sufficient for a correction factor in [7]. To ensure as close to constant gain is achieved with CgLp, the corner frequency of GFORE uses $\omega_{r\alpha} = \alpha\omega_r$. The value of α can be found in [7] for different values of γ. In [7], CgLp was also studied with the combination of a Generalized SORE and a second-order lead filter, but in this paper, only GFORE CgLp is discussed.

B. CgLp-PID

CgLp is combined with PID in [7] to obtain CgLp-PID as shown in Fig. 4. The transfer function of series PID is given in (11).

$$PID = K\left(1 + \frac{\omega_i}{s}\right)\left(\frac{1 + \frac{s}{\omega_t}}{1 + \frac{s}{\omega_d}}\right)\left(\frac{1}{1 + \frac{s}{\omega_f}}\right) \tag{11}$$

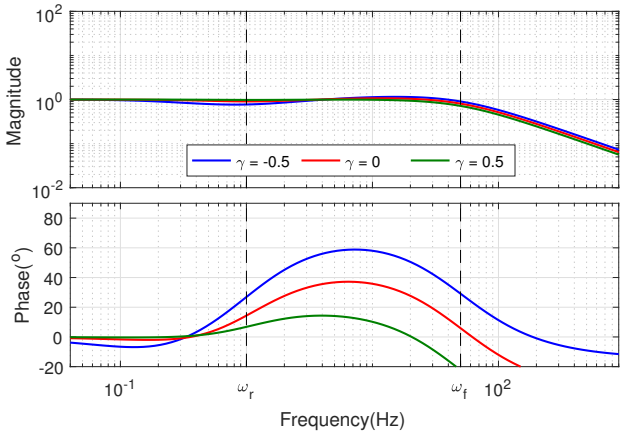

Fig. 3: Frequency response of CgLp, $\omega_r = 1$Hz

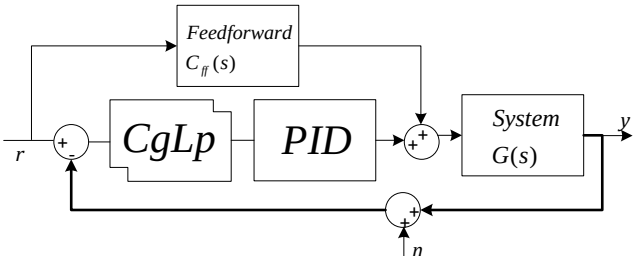

Fig. 4: Block diagram of implemented control scheme

Where K is the gain of the controller, ω_i is the frequency at which integrator action ends, ω_d and ω_t are frequencies where differentiator action starts and is terminated, and ω_f is the corner frequency of low pass filter. In general, ω_d and ω_t are chosen such that $\omega_d = \omega_c/a$ and $\omega_t = a\omega_c$ to ensure that maximum phase achieved by the differentiator is at ω_c. To increase phase margin with PID, the value of a should be increased which results in the gain at low frequencies reduces and increases at high frequencies. The combination of CgLp and PID overcomes the limitation of linear controller since CgLp adds phase without compromising the gain.

Following are the design steps adapted from [7] that is taken to design of CgLP-PID controller provided the required bandwidth (ω_c) and phase margin (PM).

1) Set the value of ω_i to be $\omega_c/10$, and ω_f to be $10\omega_c$
2) Choose value of $\omega_r < \omega_c$ and $\gamma \in [0, 1]$
3) Calculate phase added by CgLp at ω_c with describing function analysis as Ph_r
4) Set value of ω_d and ω_t such that derivative action provides phase of Ph_d at ω_c which is
$$Ph_d = PM - Ph_r$$
5) Set the value of K to obtain unity gain at ω_c.

The value of K, ω_i, and ω_f are determined using the rule of thumb of PID given in [16], while ω_d and ω_t are determined to complement phase margin requirement. Since some of the phase required is provided by CgLp, the differentiator band will be smaller than in the linear case and hence open loop shape is improved.

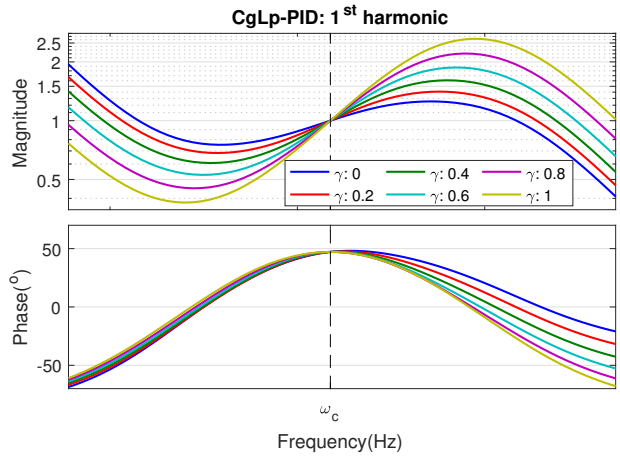

(a)

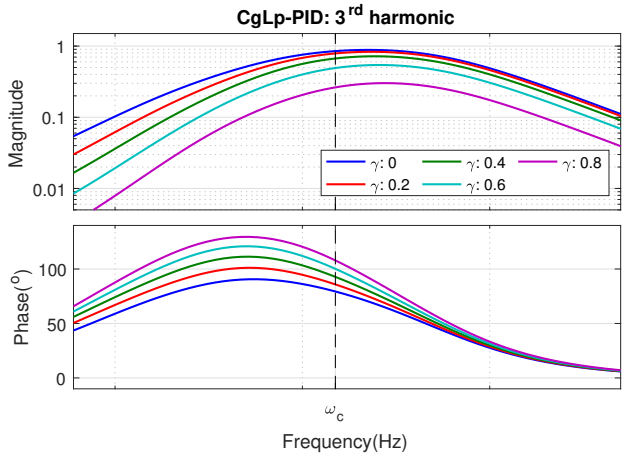

(b)

Fig. 5: Varied γ CgLp-PID (PM: 50^o, and ω_r : $\frac{\omega_c}{6}$) (a) Describing function (b) 3^{rd} order HOSIDF

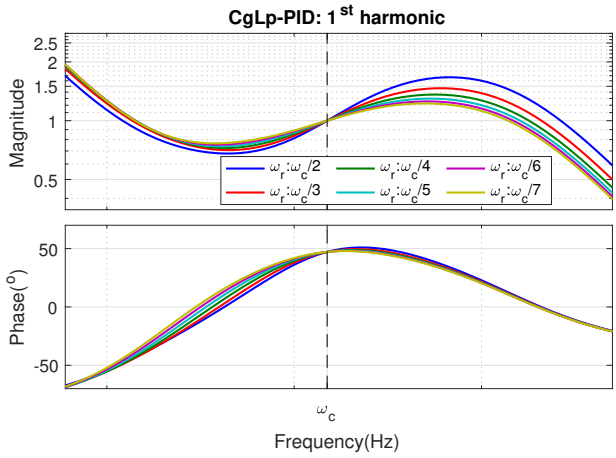

(a)

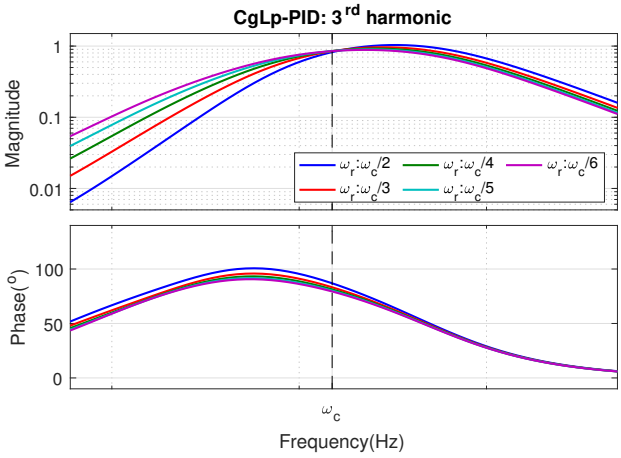

(b)

Fig. 6: Shifted ω_r CgLp-PID (PM: 50^o, and γ: 0) (a) Describing function (b) 3^{rd} order HOSIDF

C. Frequency behaviour of CgLp-PID

This subsection analyzes the frequency behaviour of CgLp-PID using describing function and HOSIDF. In literature, describing function has been used to design reset controllers, but the presence of higher order harmonic is not considered. Thus, analysis with HOSIDF might provide more insight into the performance of reset element. This analysis deals with the change of CgLp behaviour with respect to changes in design parameters γ and ω_r.

The describing function of CgLp-PID controllers which add 50^o of phase at bandwidth ω_c is shown in Fig. 5a and 6a. Fig. 5a shows CgLp-PID for different values of γ and Fig. 6a for different ω_r values. The 3^{rd} harmonic behaviour of the controllers is obtained through HOSIDF analysis and shown in Fig. 5b and 6b respectively. For simplicity, gain of controllers is normalized as if $K = 1$. From these figures, the effect of varying Cglp parameters is observed as follows:

- Lowering γ: The phase added by CgLp element is increased by lowering γ. Since the required phase margin is fixed, the phase that needs to be added by the differentiator in step 4 is reduced. This corresponds to an increase in gain at lower frequencies and decreased gain at higher frequencies. The magnitude of 3^{rd} harmonic on the other hand increases at all frequencies.
- Lowering ω_r: Since more phase is added by CgLp by lowering ω_r, similar behaviour change in first harmonic is seen. However, while the magnitude of 3^{rd} harmonic is increased at lower frequencies, it decreases at higher frequencies.

Since the behaviour of 5^{th} and higher harmonics is similar to that of 3^{rd}, these are not plotted in the figures. It must also be noted that the magnitude of harmonics decreases with increasing order.

Lowering either γ and ω_r yields to more phase added by CgLp at bandwidth and hence improves open loop first harmonic behaviour. However, a corresponding increase in 3^{rd} harmonic is also seen which could negatively affect system performance. In the next section, these CgLp-PID controllers are investigated in closed loop on a precision positioning stage.

IV. Performance of CgLp-PID

A. Practical setup

A precision positioning stage is used as shown in Fig. 7a. It has three actuators spaced angularly which actuate a central

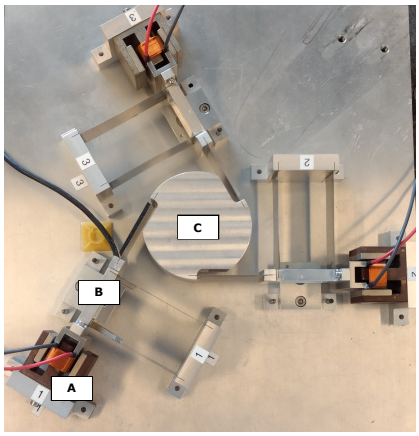

(a)

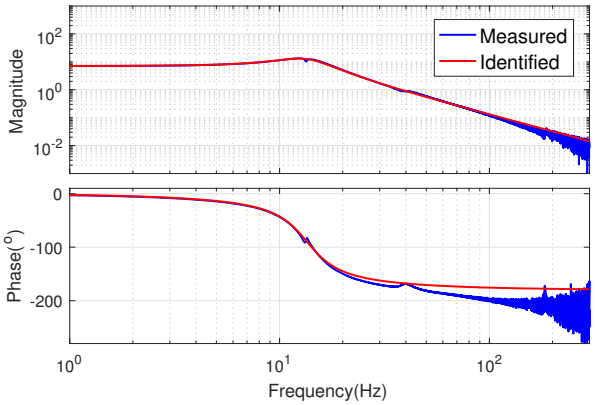

(b)

Fig. 7: (a) Picture of precision position stage actuated by Lorentz actuators with encoder and mass of interest at B. (b) Frequency response and identified model of the system

mass (C) in 3 DOF. Leaf flexures are used to suspend the masses and provide the required stiffness. Since we are concerned with SISO controller design, only one actuator (A) is utilized to control the position of mass B, resulting in a SISO system. Using Mercury M2000 linear encoder, the position of mass B is measured with the resolution of $100nm$. The controller is implemented on FPGA NI CompactRIO.

Fig. 7b shows the frequency response of the system obtained by inputting a chirp signal. The system can be approximated as a second order transfer function provided as follows.

$$G(s) = \frac{49880}{s^2 + 46s + 7189} \tag{12}$$

B. Experiment - tracking and steady state precision

This experiment is carried out to analyze trajectory tracking and steady state precision performance of CgLp-PID on the practical setup. Several CgLp-PID controllers are designed for this purpose by varying the values of γ and ω_r using the steps provided in the previous section. The controllers are again designed with a bandwidth of $\omega_c = 150Hz$ and PM of 50^o. The value of γ is varied from from 0 to 1 in steps of 0.2. For ω_r, it is varied through scale d as $\omega_r = \frac{\omega_c}{d}$ with d varied

TABLE I: RMS tracking error of system (in nm) over parameter γ and ω_r

	γ					
ω_r	0	0.2	0.4	0.6	0.8	1
$\omega_c/2$	135.9	128.0	124.1	122.0	123.7	136.7
$\omega_c/3$	132.3	126.2	117.8	116.2	119.6	136.6
$\omega_c/4$	132.8	123.9	117.6	113.6	117.1	136.6
$\omega_c/5$	131.4	123.7	118.5	116.1	118.3	136.7
$\omega_c/6$	133.2	123.7	117.5	116.7	117.3	136.5
$\omega_c/7$	132.9	124.1	122.7	118.1	117.5	136.3
$\omega_c/8$	133.5	125.0	120.9	117.9	120.3	136.2
$\omega_c/9$	135.8	127.1	124.9	120.9	121.1	136.5
$\omega_c/10$	139.9	128.5	124.7	123.2	122.2	136.8

TABLE II: RMS steady state error (in nm) of system over parameter γ and ω_r

	γ					
ω_r	0	0.2	0.4	0.6	0.8	1
$\omega_c/2$	626.7	574.6	548.4	542.6	586.5	991.3
$\omega_c/3$	589.5	569.8	546.2	555.3	637.5	991.8
$\omega_c/4$	544.9	526.9	517.0	567.5	669.1	995.3
$\omega_c/5$	522.5	503.6	506.3	552.7	638.4	993.3
$\omega_c/6$	489.2	469.3	486.8	544.3	653.1	996.9
$\omega_c/7$	475.4	479.2	478.9	509.0	632.6	994.2
$\omega_c/8$	471.1	447.2	475.8	506.8	631.9	992.5
$\omega_c/9$	463.6	442.1	466.0	518.4	623.2	993.8
$\omega_c/10$	455.7	437.5	462.9	522.4	632.1	994.7

2 to 10 in steps of 1. The controllers are implemented with a sampling frequency of $10kHz$ along with a feedforward controller C_{ff} as depicted in Fig. 4. The feedforward is the inverse of system G in (12) made proper using a second order low pass filter as given in (13).

$$C_{ff}(s) = \frac{1}{G(s)} \frac{\omega_{ff}^2}{s^2 + \omega_{ff} s + \omega_{ff}^2} \tag{13}$$

Where ω_{ff} is set to be $10\omega_c$. Note that while it is assumed that the positioning system is linear, nonlinearities are noticed in the leaf flexures resulting in a less than perfect feedforward.

For tracking analysis, the input reference uses a triangular wave signal that is based on a fourth order trajectory as explained in [17]. The precision analysis, on the other hand, uses zero value reference and applies additional white noise with a maximum amplitude of $5000nm$ at the location shown in Fig. 4. RMS of error is calculated in both cases and provided in Table I for tracking and Table II for steady state precision. In both tables, γ = 1 refers to traditional PID.

The results in Table I indicates CgLp-PID ($\gamma < 1$) outperforms traditional PID for most values of ω_r and γ. However, it is also noticed that this performance improvement is not consistent with the analysis using describing function in the previous section. Although lowering γ and lowering ω_r are both expected to improve tracking performance, deterioration in performance is seen and further it is also noticed that the performance is worse than PID for some values. Hence, this

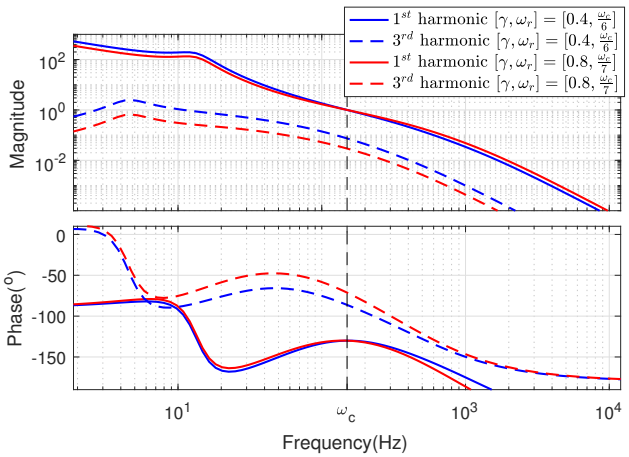

Fig. 8: 1^{st} and 3^{rd} harmonics open loop of two controllers that have similar tracking performance

deterioration in tracking performance may be caused by the rise of higher order harmonics which has been pointed out by the HOSIDF.

Table II shows that all CgLp-PID controllers surpass PID in terms of precision. However, again an interesting trend is noticed. While in describing function analysis, precision is also expected to improve for both lowering γ and lowering ω_r, the smallest error is not found for $\gamma = 0$. However in some columns, smallest error is seen for $\frac{\omega_c}{10}$.

An interesting feature is shown by the comparison of two controllers with parameter of $[\gamma, \omega_r] = [0.4, \frac{\omega_c}{6}]$ and $[\gamma, \omega_r] = [0.8, \frac{\omega_c}{7}]$. Both controllers have similar tracking error but different steady state error. Fig. 8 shows the describing function and HOSIDF of complete system open loop for both controllers. It can be seen that while one controller has better 1^{st} harmonic shape than the other, its higher harmonic gain is higher. This explains the similarity in tracking performance since the first harmonic shape improves performance while the third harmonic deteriorates performance and hence nullifies the advantage obtained in first harmonic. It is also noticed that the difference between first and third harmonic magnitude gets larger at higher frequencies resulting in a decreased influence of the third harmonic at higher frequencies. This again explains the difference seen in precision error values. Although at high frequencies, similar pattern as for tracking holds, since the magnitude of the third harmonic is significantly lower, the deteriorating effect is lesser in this case than in tracking and hence the first controller provides better precision error.

From these experiments we can say that HOSIDF has shown its benefit by showing that higher harmonics have to be considered in the design of a CgLp-PID controller. Since it is noticed that the higher order harmonics deteriorate performance, it can be said that the best CgLp-PID controller provides the best possible shape in the first harmonic while ensuring that magnitude of higher order harmonics is small enough.

C. Analysis

This subsection presents a more detailed analysis of the results obtained. Since there are no tools to relate open loop

TABLE III: Scale a of lead-lag filter of PID required for complement the phase at ω_c

	γ					
ω_r	0	0.2	0.4	0.6	0.8	1
$\omega_c/2$	1.69	1.92	2.19	2.52	2.95	3.56
$\omega_c/3$	1.48	1.72	2.02	2.39	2.88	3.56
$\omega_c/4$	1.39	1.63	1.94	2.33	2.85	3.56
$\omega_c/5$	1.33	1.58	1.89	2.3	2.83	3.56
$\omega_c/6$	1.29	1.54	1.86	2.28	2.82	3.56
$\omega_c/7$	1.27	1.52	1.84	2.26	2.81	3.56
$\omega_c/8$	1.25	1.5	1.83	2.25	2.81	3.56
$\omega_c/9$	1.23	1.49	1.81	2.24	2.81	3.56
$\omega_c/10$	1.22	1.48	1.81	2.24	2.8	3.56

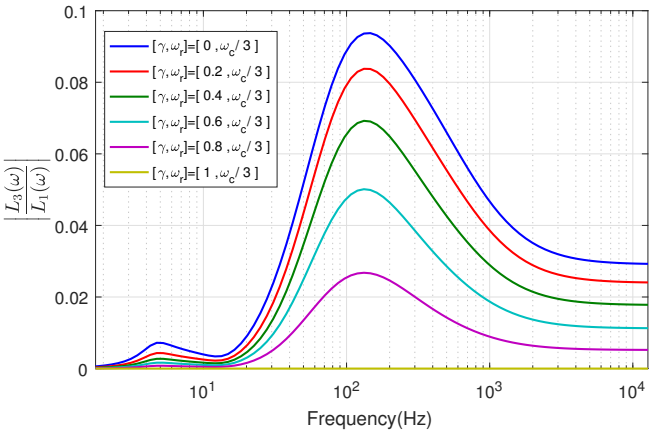

Fig. 9: Normalized 3^{rd} order harmonic

frequency behaviour of the first harmonic or higher order harmonics to closed loop system performance, the following method is used to analyze the results.

First, we assume that the describing function behaviour is not an approximation but rather accurate. In this scenario, changing value of γ and/or ω_r results in different amounts of phase added by CgLp resulting in different values of scale a of differentiator to obtain the same phase margin. The value of a for variation of γ and ω_r are respectively given in Table III. Lower value of a results in better open loop shape and hence better tracking and precision. This value of a can be used as an indicator of the expected improvement in performance. As seen from the results, this assumption is not true for all values of γ and ω_r.

So, in the second step, we consider the third harmonic and assume that this along with other higher order harmonics affect system performance negatively. However, instead of comparing the third harmonic behaviour directly, we normalize the third harmonic of open loop $L_3(\omega)$ against the first harmonic $L_1(\omega)$ for each case and compare them as shown for a few select controllers with $\omega_r = \omega_c/3$ and different values of γ in Fig. 9. From this, we calculate the maximum gain value of normalized 3^{rd} harmonic as δ. The values of δ for variation of γ and ω_r are shown in Table IV.

It is seen that δ is higher when a is lower as expected. Clearly there is a trade-off where reducing the value of a

TABLE IV: Maximum gain of normalized 3^{rd} harmonic

	γ					
ω_r	0	0.2	0.4	0.6	0.8	1
$\omega_c/2$	0.09	0.08	0.06	0.04	0.02	0.00
$\omega_c/3$	0.09	0.08	0.07	0.05	0.03	0.00
$\omega_c/4$	0.09	0.09	0.07	0.05	0.03	0.00
$\omega_c/5$	0.09	0.09	0.08	0.06	0.03	0.00
$\omega_c/6$	0.10	0.09	0.08	0.06	0.03	0.00
$\omega_c/7$	0.10	0.09	0.08	0.06	0.03	0.00
$\omega_c/8$	0.10	0.09	0.08	0.06	0.03	0.00
$\omega_c/9$	0.10	0.09	0.08	0.06	0.03	0.00
$\omega_c/10$	0.10	0.09	0.08	0.06	0.03	0.00

results in improved performance until the point where the high order harmonics are large enough to deteriorate performance. In order to achieve an optimum system performance, δ should not too high so the nonlinearity is kept low while at the same time large enough so the advantage of nonlinearity can be obtained. In this problem where $\gamma \in [0, 1]$ and $\omega_r \in \left[\frac{\omega_c}{10}, \frac{\omega_c}{2}\right]$, the highest value of δ obtained is 0.10 so it is safe to say that the optimum performance can be obtained around the half value of δ. Table I shows the tracking reaches its optimum value at value of $[\gamma, \omega_r] = [0.6, \frac{\omega_c}{/4}]$ and hence, the assumption is confirmed since from Table IV δ value of 0.05 is obtained at γ of 0.6 and ω_r of $\frac{\omega_c}{3}$ and $\frac{\omega_c}{4}$.

Therefore, from above observations following design guideline for CgLp is proposed.

- Design a PID using the rule of thumb and choose as a benchmark
- Use describing function to choose γ and ω_r that has better shape than traditional PID
- Check the value of higher order harmonics using HOSIDF and calculate the maximum gain of normalized 3^{rd} harmonic δ and ensure chosen δ is around the half of maximum possible value of δ.

V. Conclusion

The advantage of reset control in overcoming limitations of linear control have been shown in literature. Its compatibility with the PID framework combined with the use of describing function for loop shaping make it industry compatible. While most works in literature have concentrated on phase lag reduction advantage, the reset 'Constant in gain Lead in phase' filter has been used to provide broadband phase compensation and has been shown to improve system performance. However, only describing function analysis has been used for designing these controllers till date and hence better analysis of these controllers has not been possible.

In this paper, the performance of CgLp-PID on a practical precision positioning setup is analysed using both describing function and HOSIDF to account for all harmonics. It is seen that in several cases while the first harmonic behaviour indicates performance improvement to be expected, the third harmonic points in the opposite direction. Through an analysis of the designed controllers, some design guidelines are provided for the design of these CgLp-PID controllers.

Although this analysis has provided useful insight, only guidelines are provided since the exact amount of influence that these higher order harmonics have on performance is not known. Further it is necessary to validate these findings on a different system and possible different class of systems where CgLp-PID is applicable. Ideally, a complete mathematical relation between the open loop responses and closed loop system behaviour for all reset controllers is required and is part of future work.

References

[1] K. Åström and T. Hägglund, "The future of PID control," *Control Engineering Practice*, vol. 9, no. 11, pp. 1163–1175, 11 2001. [Online]. Available: https://www.sciencedirect.com/science/article/pii/S0967066101000624

[2] A. Banos, J. Carrasco, and A. Barreiro, "Reset Times-Dependent Stability of Reset Control Systems," *IEEE Transactions on Automatic Control*, vol. 56, no. 1, pp. 217–223, 2011. [Online]. Available: http://ieeexplore.ieee.org/document/5605653/

[3] J. C. Clegg, "A nonlinear integrator for servomechanisms," *Transactions of the American Institute of Electrical Engineers, Part II: Applications and Industry*, vol. 77, no. 1, pp. 41–42, 1958. [Online]. Available: http://ieeexplore.ieee.org/document/6367399/

[4] I. Horowitz and P. Rosenbaum, "Non-linear design for cost of feedback reduction in systems with large parameter uncertainty," *International Journal of Control*, vol. 21, no. 6, pp. 977–1001, 6 1975. [Online]. Available: http://www.tandfonline.com/doi/abs/10.1080/00207177508922051

[5] Y. Guo, Y. Wang, and L. Xie, "Frequency-domain properties of reset systems with application in hard-disk-drive systems," *IEEE Transactions on Control Systems Technology*, vol. 17, no. 6, pp. 1446–1453, 2009.

[6] L. Hazeleger, M. Heertjes, and H. Nijmeijer, "Second-order reset elements for stage control design," in *2016 American Control Conference (ACC)*. IEEE, 7 2016, pp. 2643–2648. [Online]. Available: http://ieeexplore.ieee.org/document/7525315/

[7] N. Saikumar, R. K. Sinha, and S. H. Hosseinnia, " Constant in gain Lead in phase element - Application in precision motion control," no. 1, pp. 1–9.

[8] Y. Li, G. Guo, and Y. Wang, "NONLINEAR MID-FREQUENCY DISTURBANCE COMPENSATION IN HARD DISK DRIVES," *IFAC Proceedings Volumes*, vol. 38, no. 1, pp. 31–36, 1 2005. [Online]. Available: https://www.sciencedirect.com/science/article/pii/S1474667016372299

[9] H. Li, C. Du, Y. Wang, and Y. Guo, "Discrete-Time Optimal Reset Control for Hard Disk Drive Servo Systems," *IEEE Transactions on Magnetics*, vol. 45, no. 11, pp. 5104–5107, 11 2009. [Online]. Available: http://ieeexplore.ieee.org/document/5297560/

[10] H. Li, C. Du, and Y. Wang, "Optimal Reset Control for a Dual-Stage Actuator System in HDDs," *IEEE/ASME Transactions on Mechatronics*, vol. 16, no. 3, pp. 480–488, 6 2011. [Online]. Available: http://ieeexplore.ieee.org/document/5752858/

[11] Y. Li, G. Guo, and Y. Wang, "Reset Control for Midfrequency Narrowband Disturbance Rejection With an Application in Hard Disk Drives," *IEEE Transactions on Control Systems Technology*, vol. 19, no. 6, pp. 1339–1348, 11 2011. [Online]. Available: http://ieeexplore.ieee.org/document/5639061/

[12] L. Chen, N. Saikumar, S. Baldi, and S. H. HosseinNia, "Beyond the Waterbed Effect: Development of Fractional Order CRONE Control with Non-Linear Reset," 5 2018. [Online]. Available: http://arxiv.org/abs/1805.10037

[13] A. Palanikumar, N. Saikumar, and S. H. HosseinNia, "No More Differentiator in PID:Development of Nonlinear Lead for Precision Mechatronics," 5 2018. [Online]. Available: http://arxiv.org/abs/1805.09703

[14] N. Saikumar, R. K. Sinha, and S. Hassan HosseinNia, "Resetting disturbance observers with application in compensation of bounded nonlinearities like hysteresis in piezo-actuators," *Control Engineering Practice*, vol. 82, pp. 36–49, 1 2019. [Online]. Available: https://linkinghub.elsevier.com/retrieve/pii/S0967066118306105

[15] K. Heinen, "Frequency analysis of reset systems containing a Clegg integrator: An introduction to higher order sinusoidal input describing functions," 2018. [Online]. Available: https://repository.tudelft.nl/islandora/object/uuid:ccc37af2-fcbc-46ec-9297-afdc5c1ea4b5?collection=education

[16] R. M. Schmidt and IOS Press., *The design of high performance mechatronics : high-tech functionality by multidisciplinary system integration*.
[17] P. F. Lambrechts, "Trajectory planning and feedforward design for electromechanical motion systems," Tech. Rep. [Online]. Available: https://pure.tue.nl/ws/files/4362785/614692.pdf

5

CONCLUSION

5.1. GENERAL CONCLUSION

The research goal of this thesis was established as follow:

To obtain tuning rules for reset controllers through analysis by describing function and HOSIDF

Based on this goal, the study is conducted using the 'Constant in phase Lead in phase' element which has been proven in literature to improve performance. However, since the improvement in performance is not explained completely using describing function analysis, this thesis has attempted to utilize higher order harmonics behaviour obtained from HOSIDF to more accurately study and explain the obtained results.

The study compares the closed loop tracking and precision performance obtained on a precision positioning stage with first and third harmonic of open loop. While phase added through CgLp results in better first harmonic shape, the same also increases magnitude of third harmonic. From observation it is concluded that the normalized gain of third harmonic should have its maximum value at around the value of maximum possible value of the normalized gain of third harmonic. Finally, it is argued that describing function and HOSIDF can be used together to design a reset controller using the provided guideline.

5.2. RECOMMENDATION

From the observations during the work of this thesis, some recommendations are given for further research which mainly serves to validate the observations of effect of higher order harmonics.

5.2.1. USE DIFFERENT PRECISION MOTION SETUP

This thesis only uses one precision motion setup to observe the effect of higher order harmonics on system performance. While this seems promising, more observations on a different setup is needed to validate the observation.

5.2.2. USE DIFFERENT CLASS OF RESET CONTROL FOR PERFORMANCE ANALYSIS

This thesis used CgLp GFORE for the observation. From literature, CgLp can be based on GSORE as well and this results in different frequency behavior of first and higher order harmonics since one more variable is introduced in CgLp GSORE as shown in Section 2. This CgLp-GSORE can be generalized further by only resetting one state of GSORE instead of all. This also results in different shape of frequency response in describing function and HOSIDF. Although this will add more complexity to the system design. Analysis with GSORE CgLp is necessary to validate the tuning guidelines obtained in this thesis.

5.2.3. CLOSED LOOP SYSTEM FREQUENCY ANALYSIS

Although this thesis provides some basic guidelines for tuning reset controllers with CgLp, complete tuning rules need to be established by finding the exact relation between open loop and closed loop frequency responses.

A

OPTIMAL TUNING FORMULATION

This appendix gives the formulation of optimal tuning in this thesis. This thesis is interested with tuning problem of controller CgLp-PID. Consider a closed loop system with a controller C and a plant P, as shown by Fig. A.1.

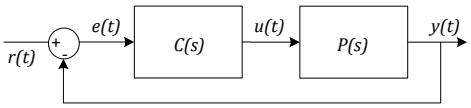

Figure A.1: Closed loop system

The optimization of the CgLp-PID for the system in Fig. A.1 is formulated as follows.

$$J(r,y) = \sqrt{\frac{1}{N}\sum_{i=1}^{N}(r-y)^2}$$

Subject to:

Describing function equation HOSIDF equation

HOSIDF equation

$$\left|\int_0^{\omega_c} C(\omega_r,\gamma,s)\right| d\omega > \left|\int_0^{\omega_c} C(\omega_r,1,s)\right| d\omega$$

$$0 \le \gamma \le 1$$

$$\frac{\omega_c}{10} \le \omega_r \le \frac{\omega_c}{2}$$

where:

ω_r : bandwidth frequency(rad/s)

$$C(\omega_r,\gamma,s) = \underbrace{\frac{1}{\frac{s}{\alpha\omega_r}+1}}_{\text{reset part}}\underbrace{\left(\frac{s}{\omega_r}+1\right)K\left(1+\frac{\omega_i}{s}\right)\left(\frac{\frac{s}{\omega_t}+1}{\frac{s}{\omega_d}+1}\right)\left(\frac{s}{\omega_f}+1\right)}_{\text{non-reset part}}$$

in which the reset part is denoted by the diagonal striketrough line, and approximated by describing function. The reset part can be defined as follows:

$$\begin{cases} \dot{x}_r & = -\alpha\omega_r\left(x_r(t)+e(t)\right) & \text{if } e \neq 0 \\ x_r(t^+) & = \gamma x_r(t) & \text{if } e = 0 \\ u_r & = x_r(t) & \end{cases}$$

with,

$$\alpha \in \mathbb{R} | \alpha > 0$$

$$\omega_i = \frac{\omega_c}{m}, \quad \omega_f = m\omega_c, \quad \omega_i = \frac{\omega_c}{a}, \quad \omega_f = a\omega_c$$

$$m \in \mathbb{R} | m > 0$$

$$a = \tan\left(\frac{\pi}{4} + \frac{pi}{360^o}\left(PM - \tan^{-1}\left(180^o + \angle \frac{\left(\frac{i\omega_c}{\omega_r}+1\right)\left(1+\frac{\omega_i}{i\omega_c}\right)P(i\omega_c)}{\left(\frac{i\omega_c}{a\omega_r}+1\right)^{x_r(t^+)}\left(\frac{i\omega_c}{\omega_f}+1\right)}\right)\right)\right)$$

PM : Phase Margin(^{o})

$$K = \left|\left(\frac{\left(\frac{i\omega_c}{a\omega_r}+1\right)^{x_r(t^+)}}{\frac{i\omega_c}{\omega_r}+1}\right)\left(\frac{\frac{i\omega_c}{\omega_f}+1}{1+\frac{\omega_i}{i\omega_c}}\right)\left(\frac{\frac{i\omega_c}{\omega_d}+1}{\frac{i\omega_c}{\omega_t}+1}\right)\frac{1}{P(i\omega_c}\right|$$

B

EXPERIMENT OVERVIEW

This chapter discuss the experiment setup that is used in this thesis. At first, the plant for the experiment is described. Then, the description of experiment setup is given. Lastly, the system identification of the whole experiment setup is provided.

B.1. PLANT

The setup is a 3 degree of freedom precision stage that consists of 3 Lorentz actuators (A1, A2, A3), 3 small masses (B1, B2, B3), 3 encoders (C1, C2, C3), and a large mass in the middle (D). These 3 actuator are used to position the mass in the middle. The setup is shown in Fig. B.1. In this thesis only one actuator (A1) is used to control the position of one mass 1). Thus, the system is considered as single mass spring damper system.

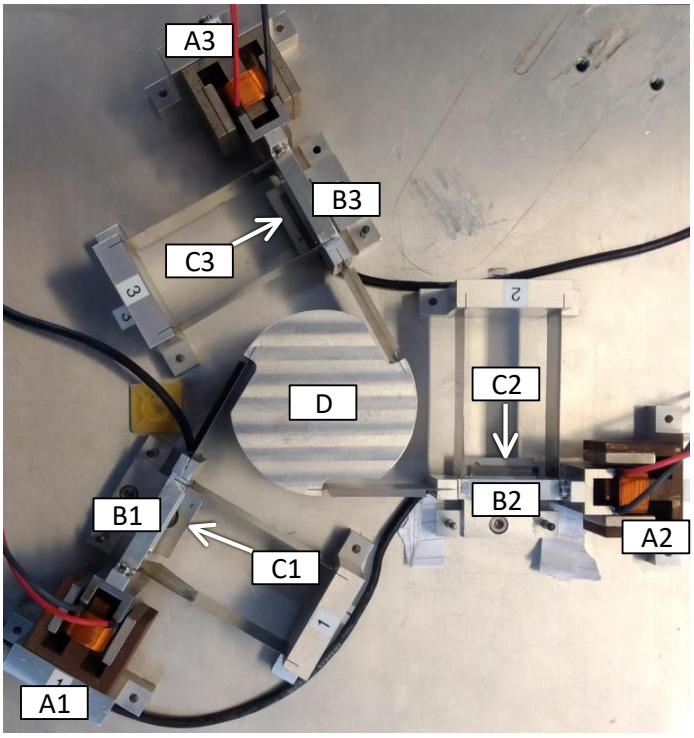

Figure B.1: 3-DOF precision stage

B.2. EXPERIMENT SETUP

The controller used National Instrument environment which consists of Labview 2016 for the software and CompactRIO for the hardware. The digital-to-analog module of CompactRIO (NI9263) sent control output to the actuator through a current amplifier. Then, the encoder signal from encoder is sent to compactRIO's digital input module (NI9401) to be computed as position data. The encoder has a resolution of 0.1 μm. A computer running labview is used to control the system in real-time. The schematic diagram of the complete control system is shown in Fig. B.2.

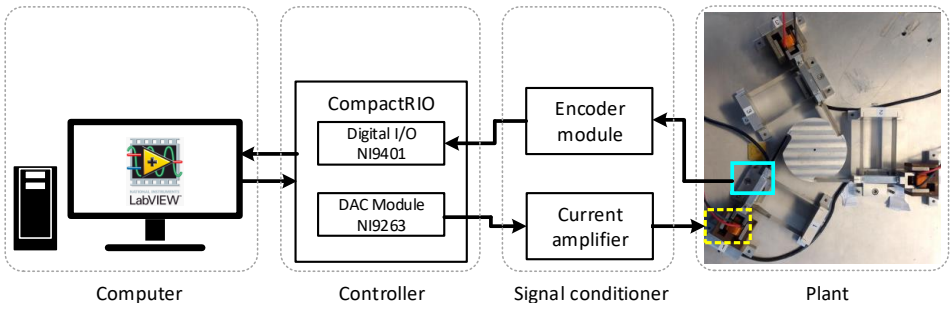

Figure B.2: Schematic of experimental setup

B.3. SYSTEM IDENTIFICATION

In order to obtain the mathematical model of the system, system identification is done by giving a chirp input signal to the system. The chirp signal composes of sine wave whose frequency is increased every second by 3% from 0.1 to 1000 Hz. The response is logged for every 10μs and the data is used to obtain transfer function of the system using *tfestimate* function by MATLAB. Fig. B.3 and Fig. B.4 respectively shows the data logging from identification process and the identified open loop frequency response of the system.

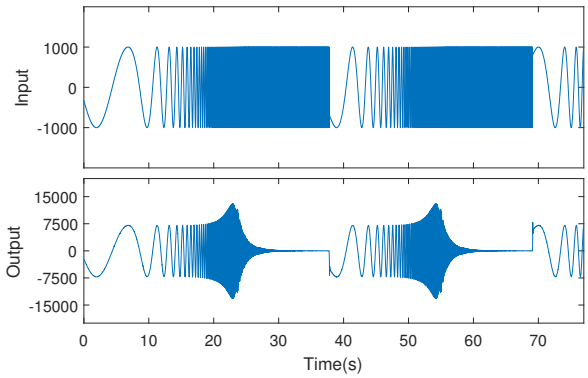

Figure B.3: Time response (output) of the plant from chirp signal(input)

From the identified frequency response, the estimated transfer function is obtained as follows.

$$P_{est}(S) = \frac{49880}{s^2 + 46s + 7189}$$

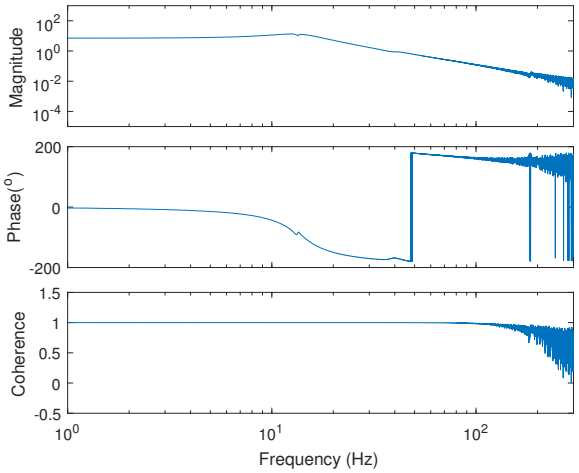

Figure B.4: Identified frequency response with coherence checked

C

Simulation Results

This appendix provides the plot results obtained during this thesis which may be useful for future works. The given plots are the normalized third order harmonics of open loop system which discussed in Section IV of the paper in Chapter 2. In summary, the improvement by CgLp is followed by the rise of higher order harmonics. Since only 2 parameters ω_r but the γ are utilized in CgLp there is not much variation shown by the plot.

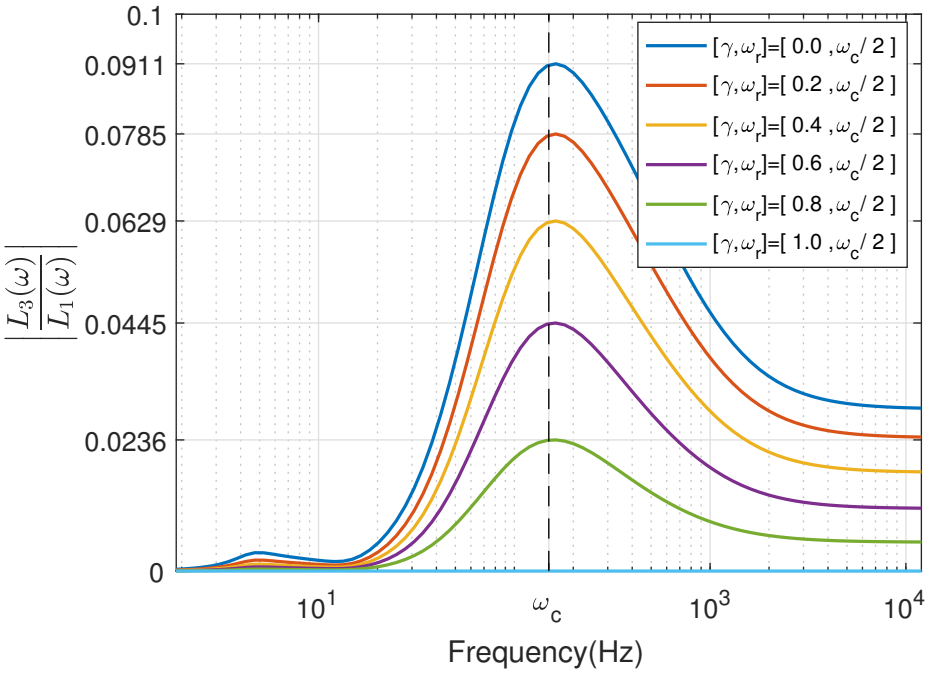

Figure C.1: Normalized third order harmonic of open loop system at $\omega_r = \frac{\omega}{2}$

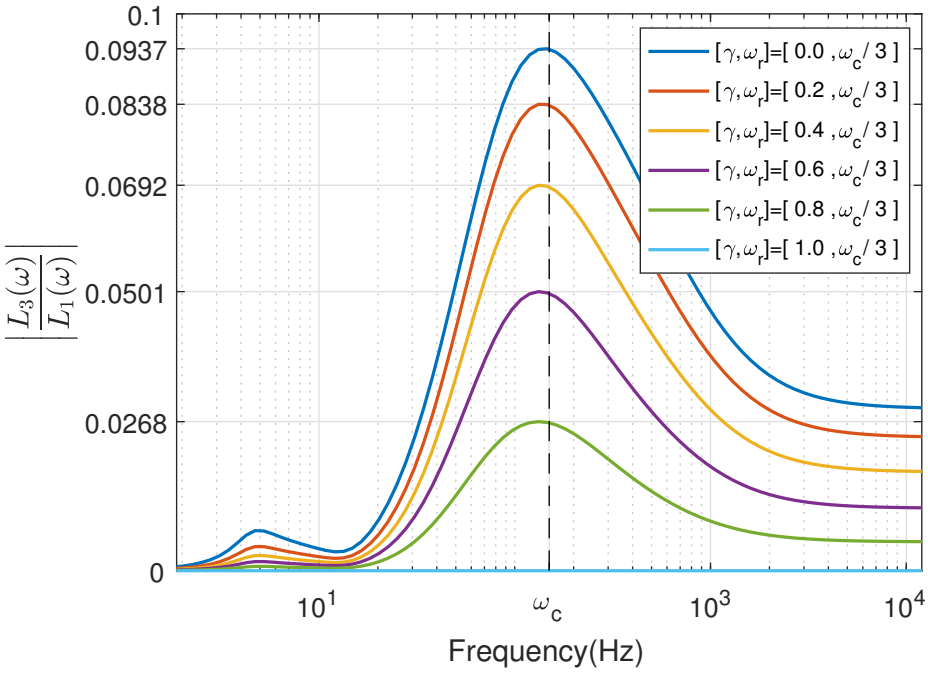

Figure C.2: Normalized third order harmonic of open loop system at $\omega_r = \frac{\omega}{3}$

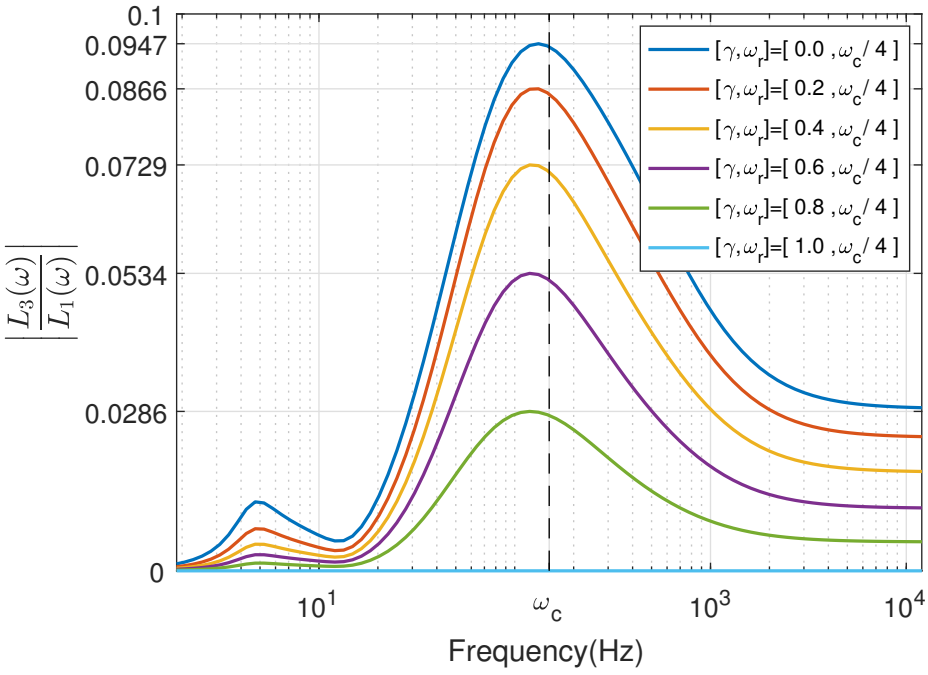

Figure C.3: Normalized third order harmonic of open loop system at $\omega_r = \frac{\omega}{4}$

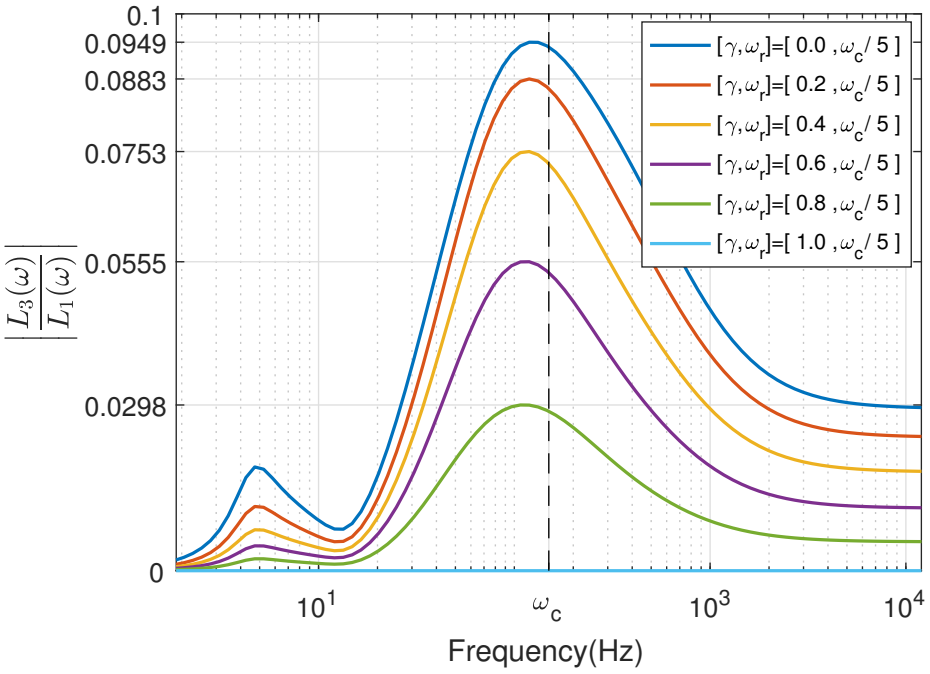

Figure C.4: Normalized third order harmonic of open loop system at $\omega_r = \frac{\omega}{5}$

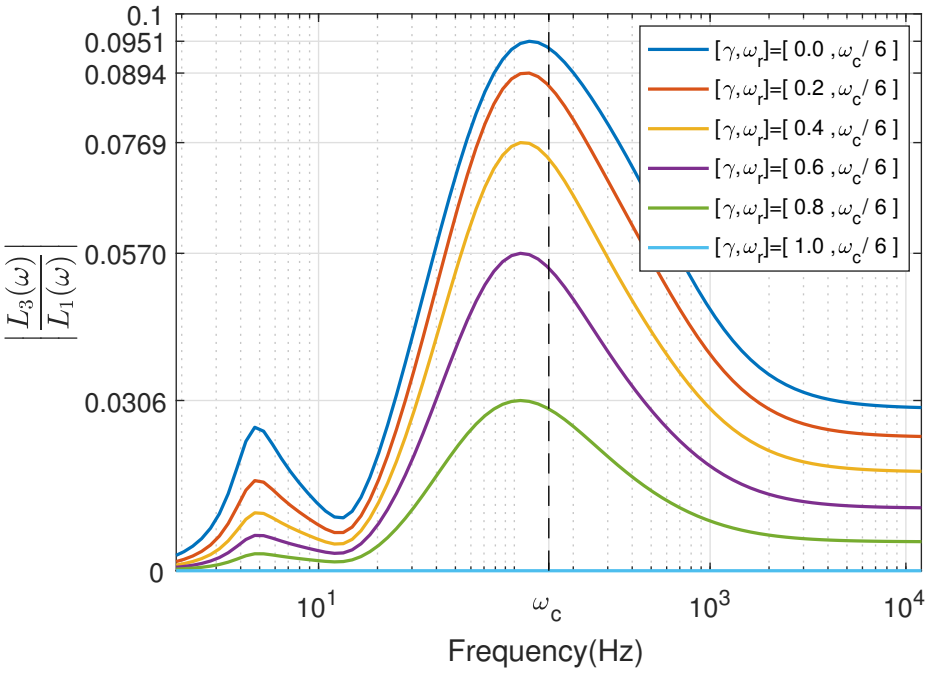

Figure C.5: Normalized third order harmonic of open loop system at $\omega_r = \frac{\omega}{6}$

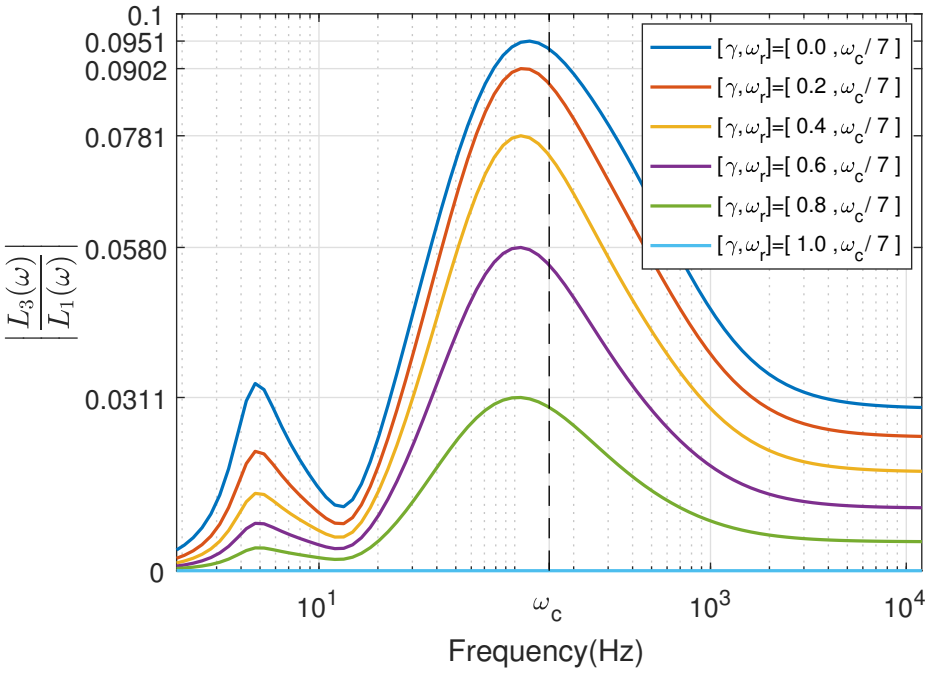

Figure C.6: Normalized third order harmonic of open loop system at $\omega_r = \frac{\omega}{7}$

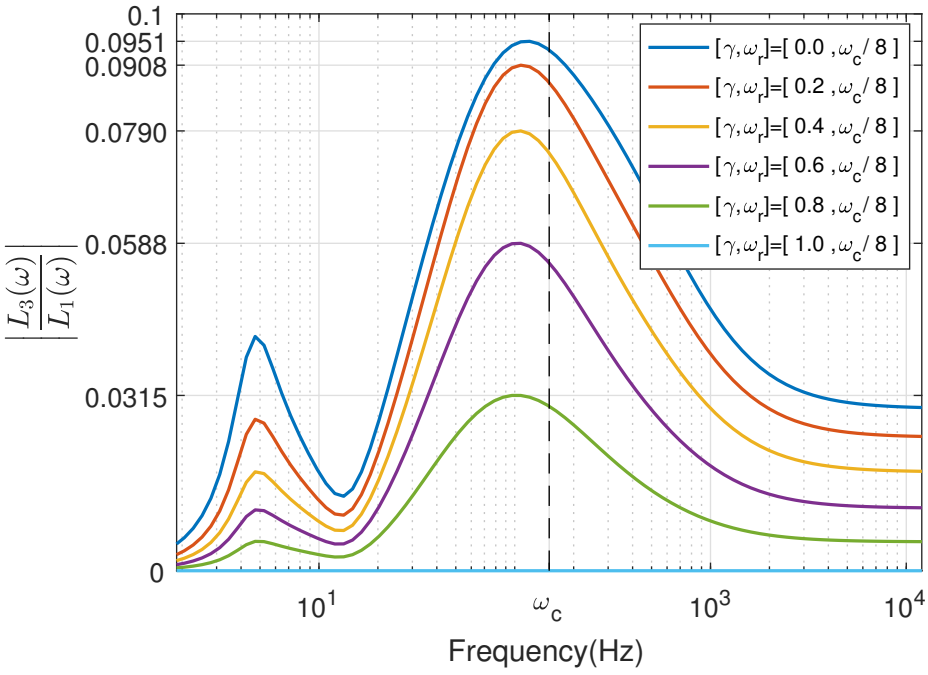

Figure C.7: Normalized third order harmonic of open loop system at $\omega_r = \frac{\omega}{8}$

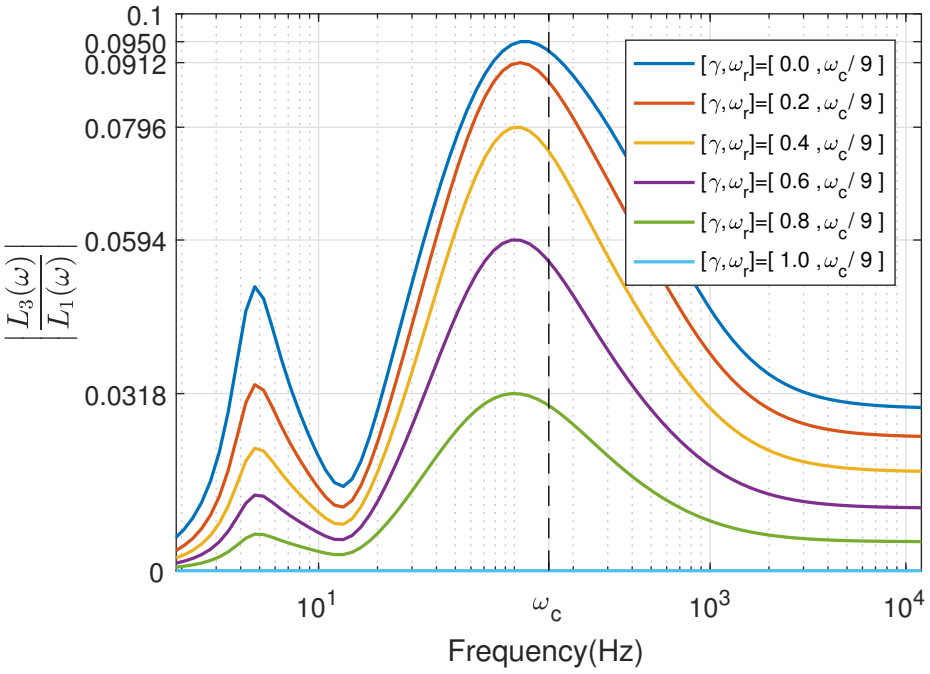

Figure C.8: Normalized third order harmonic of open loop system at $\omega_r = \frac{\omega}{9}$

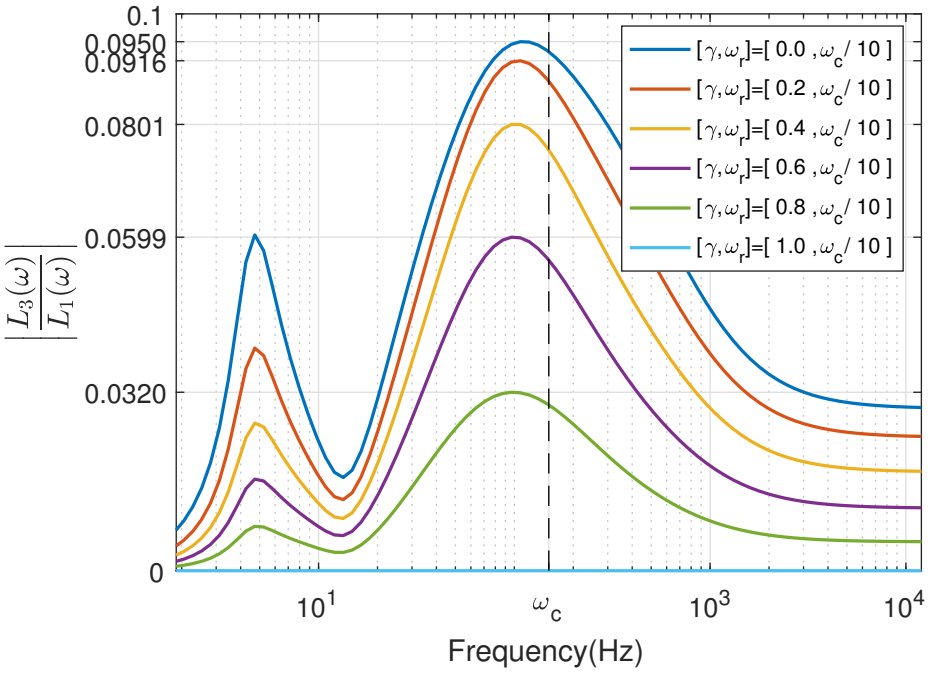

Figure C.9: Normalized third order harmonic of open loop system at $\omega_r = \frac{\omega}{10}$

D

MATLAB AND SIMULINK CODE

In this appendix, the MATLAB and SIMULINK code used in this thesis are given. The first MATLAB code is used to identify the transfer function from the data obtained from experiment. Then, the later code are the code which used to plot describing function(1^{st} and 3^{rd} order harmonics) of open loop system and the real-time simulation of the system.

D.1. IDENTIFICATION.M

```
Input  = VarName2; % acquire input data
Output = VarName3; % acquire output data

Ts     = 10e-6;    % time sampling
[Txy,F]= tfestimate(Input,Output,[],[],[],1/Ts);
[Cxy,F]= mscohere(Input,Output,[],[],[],1/Ts);

% Plot Input and Output
figure;
time = 1:size(Input,1);
time = time.*Ts;
subplot(211)
plot(time,Input)
xlim([0 max(time)]); ylabel('Input'); ylim([-2000 2000]);
set(gca,'XTickLabel',[]);
subplot(212)
plot(time,Output);
xlim([0 max(time)]); ylabel('Output'); xlabel('Time(s)');

limx   = [1 3e2];
% Plot frequency response and coherence
figure;
subplot(311)
loglog(F,abs(Txy));
ylabel('Magnitude');xlim(limx);ylim([1e-5 1e3]);set(gca,'XTickLabel',[]);
subplot(312)
semilogx(F,(rad2deg(angle(Txy))));
ylabel('Phase(^o)');xlim(limx);set(gca,'XTickLabel',[]);
subplot(313)
semilogx(F2,Cxy);
ylabel('Coherence');xlabel('Frequency(Hz)');
xlim(limx);ylim([-0.5 1.5]);
```

D.2. MAIN.M

```
%% CGLP-PID simulation
% plot 1st and 3rd order harmonic
% simulate CgLp PID in simulink to acquire tracking/precision performance
%% Initialization
clear all;
close all;
clc;
s       = tf('s');
xmin    = -4 ; xmax = 5;          % frequency plot limit
omega   = logspace(xmin,xmax,200);

%% Setup and Requirement
Ts    = 1/10e3; % sampling time in seconds
nWave = 50;     % signal wave cycle for simulation
disp  = 10000;  % wave amplitude for simulation
trajectory;     % generate trajectory for simulation

% Plant
m = 1/4.988e4; c = 46.33*m; k = 7190*m;
P = 1/(m*s^2+c*s+k);

% Requirement
w_c = 150*2*pi;   % bandwidth frequency
PM  = 50;         % required phase margin

w_i = w_c/10;                                % integrator frequency
w_f = w_c*10;                                % low pass filter frequency
lag = @(wdn,wtn) (s/wdn + 1)/(s/wtn + 1); % lag-lead filter

%% Input variable.
% number of a should be number of row of gamma array
% for GFORE gamma = [0.1; 0.2] means two controller being observed
% for GSORE gamma = [0.1 0.1;0.2 0.3;] means two controller being observed

resetelementorder = 2; % 1 for GFORE CgLp; 2 for GSORE CgLp
if resetelementorder == 1       % GFORE mode
    % Parameter value
    a       = [3 3 3];                       % a is scale for w_r=w_c/a,
    gamma   = [0.3; 0.2; 0.1];
    % Reset part of controller
    R       = @(alpha,w_r) 1/(s/(alpha*w_r)+1);
    % Non-reset part of controller
    l_c     = @(w_rn)     (s/w_rn+1)*(1+w_i/s)/(s/(w_f)+1);

elseif resetelementorder == 2   % GSORE mode
    % Parameter value
    a       = [3 3 3];                       % a is scale for w_r=w_c/a,
    gamma   = [0.6 0.6;0.5 0.5;0.4 0.4];
    % Reset part of controller
    beta_r = 0.8;
    R       = @(alpha,w_r) 1/((s/(alpha*w_r))^2+2*beta_r*s/(alpha*w_r)+1);
    % Non-reset part of controller
    l_c     = @(w_rn)     (s/w_rn+1)^2*(1+w_i/s)/(s/(w_f)+1);
end
```

```
55
56
57 % plot 1st & 3rd order harmonics
58 close all
59 [m1,p1] = bodeData(P,w_c);
60 for lt = 1:size(gamma,1)
61     w_r(lt)= w_c/a(lt);
62     strng(lt,:) =[{'[\gamma,\omega_r]=['...
63         ,num2str(gamma(lt)),',\omega_c/',num2str(a(lt)),']'}];
64
65     findAlpha;
66     G  = R(alpha(lt),w_r(lt));
67     [A_r,B_r,C_r,D_r] = ssdata(G);
68
69
70     if      size(A_r,1) == 1;  Arho = gamma(lt);
71     elseif size(A_r,1) == 2;  Arho = [gamma(lt,1) 0;0 gamma(lt,2)];
72     end
73
74     % compute d scale of lead-lag filter
75     [m2,p2] = descFunc(A_r,B_r,C_r,D_r,Arho,w_c,1);
76     [m3,p3] = bodeData(l_c(w_r(lt)),w_c);
77     phtot   = 180 + p1 + p2 + p3;
78     reqPh   = deg2rad(double(PM - phtot));
79     d       = tan((reqPh + (pi)/2)/2); % d  = 2.3316;
80     w_d(lt) = double(w_c/d);
81     w_t(lt) = double(w_c*d);
82
83     % compute gain of controller
84     [m4,p4] = bodeData(lag(w_d(lt),w_t(lt)),w_c);
85     K(lt)   = 1/(m1*m2*m3*m4);
86
87     str = strjoin((strng(lt,:)));
88     % uncomment row below see complete open loop
89     L = K(lt)*l_c(w_r(lt))*lag(w_d(lt),w_t(lt))*P;
90
91     % uncomment row below to see normalized controller
92 %     L= l_c(w_r(lt))*lag(w_d(lt),w_t(lt))/(m2*m3*m4);
93
94
95     [AL,BL,CL,DL] = ssdata(L);
96     A = [A_r zeros(size(A_r,1),size(AL,2));BL*C_r AL];
97     B = [B_r;BL*D_r];
98     C = [DL*C_r CL];
99     D = D_r*DL;
100    Arho = eye(size(A,1));
101    Arho(1:size(gamma,2),1:size(gamma,2))= gamma(lt,:);
102
103    % plot 1st order harmonic
104    figure(1); hold on
105    set(gcf, 'Position', [10 10 450 300])
106    [mRL1(lt,:),pRL1(lt,:),DFR1(lt,:)] = descFunc(A,B,C,D,Arho,omega,1);
107    [mag(lt),pha(lt)]   = freqPlot(mRL1(lt,:),pRL1(lt,:),omega,str);
108
109
110    % plot 3rd order harmonic
```

```
    figure(1); hold on
    set(gcf, 'Position', [10 10 450 300])
    [mRL3(lt,:),pRL3(lt,:),DFR3(lt,:)] = descFunc(A,B,C,D,Arho,omega,3);
    [mag3(lt),pha3(lt)] = freqPlot(mRL3(lt,:),pRL3(lt,:),omega,str);

    normDF3(lt,:) = DFR3(lt,:)./DFR1(lt,:);
    figure(3);set(gcf, 'Position', [10 10 500 300])
    semilogx(omega./(2*pi),abs(normDF3(lt,:)),'DisplayName',str,'LineWidth',1.2);
    hold on
    legend({},'FontSize',8,'FontWeight','normal','Location','best');
    ylabel('$$\left|\frac{L_3(\omega)}{L_1(\omega)}\right|$$','interpreter','latex')
        ;
    maxNorm(lt) = max(abs(normDF31(lt,:)));
    xlabel('Frequency(Hz)');
end

for k = 1:3;
    figure(k);
    if k<3;
        subplot(211);
        xlim([w_c/(2*pi)/80 w_c/(2*pi)*80]);ylim([1e-3 1e3])
        semilogx([w_c./(2*pi) w_c./(2*pi)],get(gca, 'ylim'),'k--');
        subplot(212);

        xlim([w_c/(2*pi)/80 w_c/(2*pi)*80]);
        semilogx([w_c./(2*pi) w_c./(2*pi)],get(gca, 'ylim'),'k--');
    else
        xlim([w_c/(2*pi)/80 w_c/(2*pi)*80]); ylim([0 0.1]);
        semilogx([w_c./(2*pi) w_c./(2*pi)],get(gca, 'ylim'),'k--');
    end
end

%% simulation to see tracking error or precision error
for lt = 1:size(gamma,1)
    % reset controller
    G  = R(alpha(lt),w_r(lt));
    Gd  = c2d(G,Ts,'tustin');
    [A_rd,B_rd,C_rd,D_rd] = ssdata(Gd);

    % non-reset controller
    L  = K(lt)*l_c(w_r(lt))*lag(w_d(lt),w_t(lt));
    Ld  = c2d(L,Ts,'tustin');
    [numLd,denLd] = tfdata(Ld,'v');

    % feed forward controller
    FF  = (1/P)/((s/w_f)^2+2*(s/w_f)+1);
    FFd = c2d(FF,Ts,'tustin');
    [numFF,denFF] = tfdata(FFd,'v');

    % plant
    [numP,denP] = tfdata(P,'v');

    if     size(A_r,1) == 1;  Arho = gamma(lt);
    elseif size(A_r,1) == 2;  Arho = [gamma(lt,1) 0;0 gamma(lt,2)];
    end

```

```
166     sim('cglppid');
167
168     % plot time response
169     str = strjoin((strng(lt,:)));
170     time = track.time;
171     trackData = track.signals(1).values(:);
172     trackError= track.signals(2).values(:);
173     figure(3);
174     ax1 = subplot(211);grid on;
175     plot(ax1,time,trackData(:,1),'DisplayName',str);
176     xlim(ax1,[min(time) max(time)]);
177     ylabel(ax1,'System Response(m)');
178     legend({},'FontSize',10,'FontWeight','normal','Location','best');
179     hold on
180     ax2 = subplot(2,1,2);grid on;
181     plot(ax2,time,trackError(:,1),'DisplayName',str);
182     xlim(ax2,[min(time) max(time)]);
183     ylabel(ax2,'Error(m)'); xlabel(ax2,'Time(s)');
184     hold on;
185     rms_error(lt) = sqrt(mean((err_discrete(:,:).^2)));
186 end
187 rms_error(lt)
```

D.3. TRAJECTORY.M

```
td = 400;
tj = 400;
ta = 400;
tv = 400;
d = zeros(1,tj/4);
d = horzcat(d,ones(1,td));
d = horzcat(d,zeros(1,tj));
d = horzcat(d,-1*ones(1,td));
d = horzcat(d,zeros(1,ta));
d = horzcat(d,-1*ones(1,td));
d = horzcat(d,zeros(1,tj));
d = horzcat(d,ones(1,td));
d = horzcat(d,zeros(1,tv));
d = horzcat(d,-1*ones(1,td));
d = horzcat(d,zeros(1,tj));
d = horzcat(d,ones(1,td));
d = horzcat(d,zeros(1,ta));
d = horzcat(d,ones(1,td));
d = horzcat(d,zeros(1,tj));
d = horzcat(d,-1*ones(1,td));
d = horzcat(d,zeros(1,tj/4));
d = d*0.001;
pindexmax = size(d,2);
j = zeros(1,size(d,2));
for i = 2:size(d,2)
j(i) = j(i-1) + d(i-1);
end
a = zeros(1,size(d,2));
for i = 2:size(d,2)
a(i) = a(i-1) + j(i-1);
end
v = zeros(1,size(d,2));
for i = 2:size(d,2)
v(i) = v(i-1) + a(i-1);
end
ref = zeros(1,size(d,2));
for i = 2:size(d,2)
ref(i) = ref(i-1) + v(i-1);
end
ref = ref/ref(end)*disp;
for i = 1:size(d,2)
ref(i) = ref(i) - mod(ref(i),1);
end
ref = ref - mod(ref,1);
ref_temp = horzcat(ref,fliplr(ref));
ref = ref_temp;
for i = 2:nWave
    ref = horzcat(ref,ref_temp);
end
time = [1:size(ref,2)].*Ts;
runtime= time(end);
ref = timeseries(ref,time,'name','trajectory');
save refer.mat -v7.3 ref
```

D.4. DESCFUNC.M

```
function [Gain,Phase] = descFunc(A_r,B_r,C_r,D_r,gamma,omega,n)
% a function to acquire gain and phase of
% describing function of system of sys(A_r,B_r,C_r,D_r)
% with size(gamma) of [1 1] for GFORE or [2 2] for GSORE
% omega : corresponding frequency
% n     : the order of harmonic(only odd number)
I = eye(size(A_r));
for j=1:length(omega)
    Lambda = omega(j)^2*I + A_r^2;
    Delta_D = I + gamma*expm(pi/omega(j)*A_r);
    Delta   = I + expm(pi/omega(j)*A_r);
    Gamma_D = Delta_D^-1 * gamma * Delta * Lambda^-1;
    Theta_D = -2*omega(j)^2 /pi * Delta *(Gamma_D - Lambda^-1);
    if n == 1
        DF(j)  = C_r*(i*omega(j)*I - A_r)^-1*(I + i*Theta_D) * B_r + D_r;
    else
        DF(j) = (-2*omega(j)^2*C_r/(i*pi))*...
            (A_r - i*omega(j)*n*I)^-1 *Delta*(Gamma_D-Lambda^-1)*B_r;
    end
end
Gain    = abs(DF);
Phase   = vpa(rad2deg(angle(DF)),4);
```

D.5. BODEDATA.M

```
function [magArray,phaseArray] = bodeData(L,omega)
% acquire magnitude and phase of transfer function of L over omega
[mag,phase] = bode(L,omega);
for i = 1 : length(omega)
    magArray(i)   = mag(i);
    phaseArray(i) = phase(i);
end
```

D.6. FREQPLOT.M

```
function [m,n] = freqPlot(Mag,Pha,omega,string)
hold on
w = omega./(2*pi); % Hz
ax1 = subplot(211);
set(gca,'fontsize',10); set(gca,'XTickLabel',[]);
m = semilogx(ax1,w,mag2db(Mag),'DisplayName',string,'LineWidth',1.5);
xlim([min(w) max(w)]);
grid on;
ylabel('Magnitude(dB)');
legend({},'FontSize',10,'FontWeight','normal','Location','best');
hold on

ax2 = subplot(212);set(gca,'fontsize',10);
n = semilogx(ax2,w,Pha,'DisplayName',string,'LineWidth',1.5);
xlim([min(w) max(w)]);
grid on;
ylabel('Phase(^o)'); xlabel('Frequency(Hz)');
hold on
```

D.7. SIMULINK FOR REAL-TIME SIMULATION

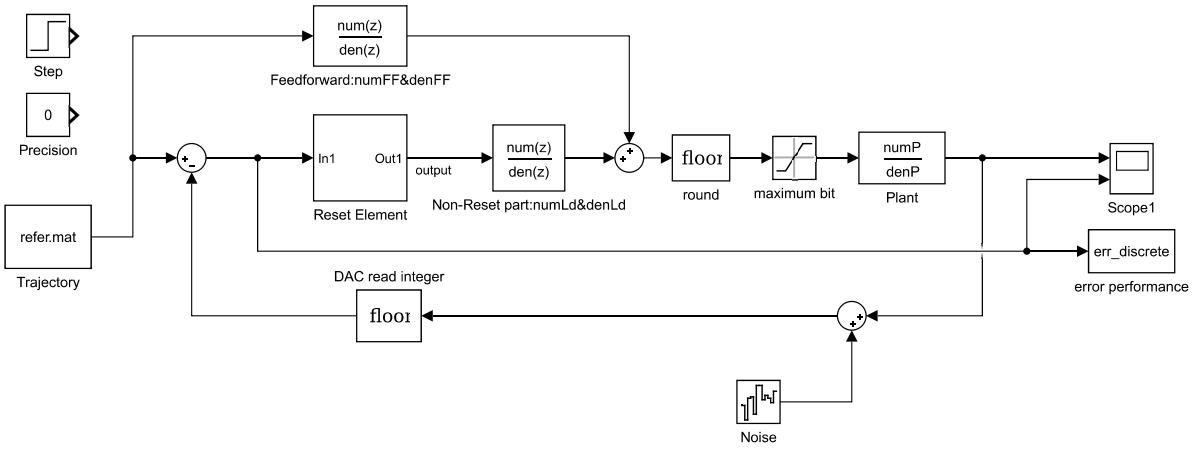

Figure D.1: Simulink schematic for real-time simulation named cglppid.slx

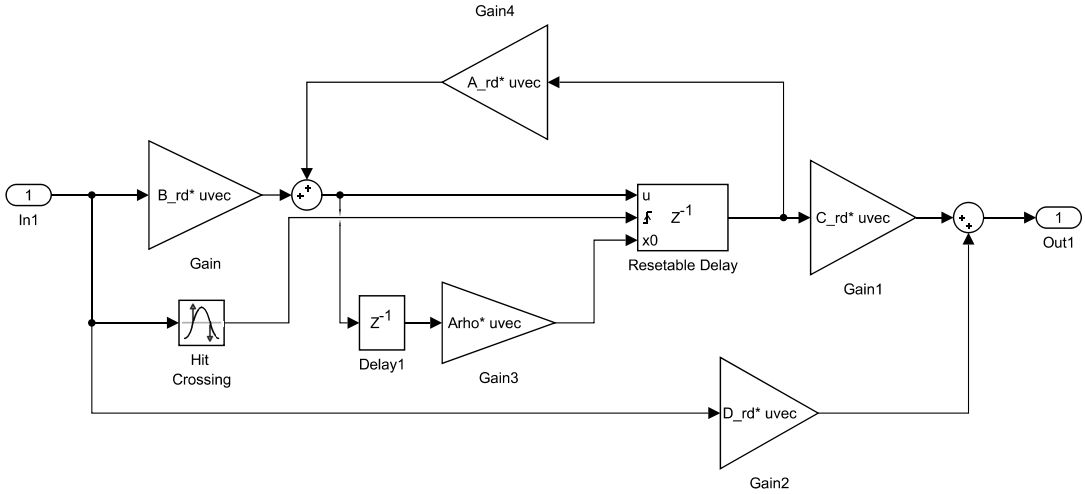

Figure D.2: Reset Element subsystem in cglppid.slx

BIBLIOGRAPHY

[1] *ASML ships new TWINSCAN NXT immersion lithography platform | Solid State Technology,* .

[2] K. Åström and T. Hägglund, *The future of PID control,* Control Engineering Practice **9**, 1163 (2001).

[3] A. Banos, J. Carrasco, and A. Barreiro, *Reset Times-Dependent Stability of Reset Control Systems,* IEEE Transactions on Automatic Control **56**, 217 (2011).

[4] J. C. Clegg, *A nonlinear integrator for servomechanisms,* Transactions of the American Institute of Electrical Engineers, Part II: Applications and Industry **77**, 41 (1958).

[5] J. Moreno, J. Guzmán, J. Normey-Rico, A. Baños, and M. Berenguel, *A combined FSP and reset control approach to improve the set-point tracking task of dead-time processes,* Control Engineering Practice **21**, 351 (2013).

[6] M. A. Davo and A. Banos, *Reset control of a liquid level process,* in *2013 IEEE 18th Conference on Emerging Technologies & Factory Automation (ETFA)* (IEEE, 2013) pp. 1–4.

[7] F. Perez, A. Banos, and J. Cervera, *Periodic reset control of an in-line pH process,* in *ETFA2011* (IEEE, 2011) pp. 1–4.

[8] M. Heertjes, K. Gruntjens, S. van Loon, N. Kontaras, and W. Heemels, *Design of a variable gain integrator with reset,* in *2015 American Control Conference (ACC)* (IEEE, 2015) pp. 2155–2160.

[9] Y. Li, G. Guo, and Y. Wang, *Reset Control for Midfrequency Narrowband Disturbance Rejection With an Application in Hard Disk Drives,* IEEE Transactions on Control Systems Technology **19**, 1339 (2011).

[10] Y. Li, G. Guo, and Y. Wang, *Phase lead reset control design with an application to HDD servo systems,* in *9th International Conference on Control, Automation, Robotics and Vision, 2006, ICARCV '06* (2006).

[11] L. Hazeleger, M. Heertjes, and H. Nijmeijer, *Second-order reset elements for stage control design,* in *2016 American Control Conference (ACC)* (IEEE, 2016) pp. 2643–2648.

[12] Y. Zheng, Y. Chait, C. Hollot, M. Steinbuch, and M. Norg, *Experimental demonstration of reset control design,* Control Engineering Practice **8**, 113 (2000).

[13] E. Delgado, M. Diaz-Cacho, A. Banos, and A. Barreiro, *Reset control of synchronous motors with permanent magnet excitation,* in *22nd Mediterranean Conference on Control and Automation* (IEEE, 2014) pp. 1347–1352.

[14] E. Delgado, A. Barreiro, M. Diaz-Cacho, and P. Falcon, *Wheel slip reset controller in automotive brake systems,* in *2014 IEEE International Electric Vehicle Conference (IEVC)* (IEEE, 2014) pp. 1–6.

[15] A. Costas, M. Cerdeira-Corujo, A. Barreiro, E. Delgado, and A. Banos, *Car platooning reconfiguration applying reset control techniques,* in *2016 IEEE 21st International Conference on Emerging Technologies and Factory Automation (ETFA)* (IEEE, 2016) pp. 1–8.

[16] N. Saikumar, R. K. Sinha, and S. H. Hosseinnia, *'Constant in gain Lead in phase' element - Application in precision motion control,* , 1.

[17] K. Heinen, *Frequency analysis of reset systems containing a Clegg integrator: An introduction to higher order sinusoidal input describing functions,* (2018).